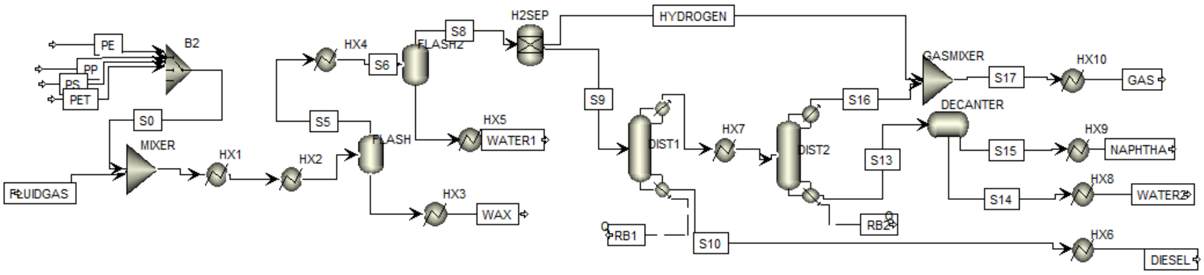

Separation of Condensable Products from Plastic Pyrolysis

Design and evaluation of separation processes and plastic waste feedstocks

Master's thesis in Sustainable Energy Systems

DANIEL HELLBERG

DEPARTMENT OF SPACE, EARTH AND ENVIRONMENT
CHALMERS UNIVERSITY OF TECHNOLOGY
Gothenburg, Sweden 2025
www.chalmers.se

Master's thesis 2025

Separation of Condensable Products from Plastic Pyrolysis

Design and evaluation of separation processes and plastic waste feedstocks

DANIEL HELLBERG

CHALMERS
UNIVERSITY OF TECHNOLOGY

Department of Space, Earth and Environment
Division of Energy Technology
Gasification group
Chalmers University of Technology
Gothenburg, Sweden 2025

Separation of Condensable Products from Plastic Pyrolysis
Design and evaluation of separation processes and plastic waste feedstocks
DANIEL HELLBERG

Supervisors: Chahat Mandviwala and Judit Fortet Casabella, Department of Space, Earth and Environment. Gabriel Gustafsson, BioShare.
Examiner: Martin Seemann, Department of Space, Earth and Environment.

Master's Thesis 2025
Department of Space, Earth and Environment
Division of Energy Technology
Gasification group
Chalmers University of Technology
SE-412 96 Gothenburg
Telephone +46 31 772 1000

Cover: Aspen Plus model of process 3.

Typeset in LaTeX
Printed by Chalmers Reproservice
Gothenburg, Sweden 2025

Separation of Condensable Products from Plastic Pyrolysis
Design and evaluation of separation processes and plastic waste feedstocks
DANIEL HELLBERG
Department of Space, Earth and Environment
Chalmers University of Technology

Abstract

The increasing generation of plastic waste and the limitations of mechanical recycling have motivated the use of thermochemical recycling methods, such as pyrolysis. The pyrolysis of plastic waste yields a mixture of waxes, pyrolysis oil and light gases that need to be separated for downstream applications like steam cracking. This thesis designs and evaluates three separation processes for isolating specific fractions from the hydrocarbon mixture, with focus on the naphtha fraction. As a tool, Aspen Plus was used to simulate the processes and optimize the process parameters for a high yield of target components for each product stream from the process. An objective is also to test the adaptability of the separation process to variable plastic waste feedstocks like polyethylene, polypropylene and mixed plastic waste. The results show that more advanced configurations using distillation columns provide better separation performance and product purity, with a slightly higher cost. From this result it was concluded that it would be more cost-beneficial to build such a process compared to a simpler process. A result was also that switching feedstock between polyethylene and polypropylene did not affect the separation efficiency negatively. However, pyrolysis products from mixed plastic waste could not be separated as efficient, mostly due to the organic acids which have their origin in polyethylene terephthalate. Alternative separation techniques would need to be explored to assess this limitation in the separation process.

Keywords: plastic pyrolysis, thermochemical recycling, separation process, naphtha, Aspen Plus, process design, feedstock variability.

Acknowledgements

There are some people that have helped me throughout my master thesis, that I want to say a special thanks to:

I would first like to thank my supervisors from Chalmers, Judit Fortet Casabella and Chahat Mandviwala, for continuously supporting me with the project and giving me feedback. I also want to thank my supervisor from BioShare, Gabriel Gustafsson, for bringing the idea of the thesis and taking his time for several supervision meetings. A thanks to my examiner Martin Seemann for grading this thesis, and hopefully approving it.

A special thanks to the whole Gasification group at the Division of Energy Technology at Chalmers, that gave me both feedback on my presentations and interesting discussions throughout the project.

Lastly I would like to thank the guy sitting next to me when I was writing my thesis, Luis Enrique Anaya Aguilar, for having many discussions and for helping each other throughout our master thesises.

Daniel Hellberg, Gothenburg, June 2025

List of Acronyms

Below is the list of acronyms that have been used throughout this thesis listed in alphabetical order:

CAPEX	Capital Expenses
DKR	Deutsche Kunststoff Recycling
DSTWU	Distillation Shortcut Winn-Underwood-Gill method
GC	Gas Chromatography
GCC	Grand Composite Curve
HDPE	High Density Polyethylene
HHV	Higher Heating Value
HP	High Pressure
ISBL	Inside Battery Limits
LP	Low Pressure
MP	Medium Pressure
OPEX	Operational Expenses
PE	Polyethylene
PET	Polyethylene terephthalate
PINA	n-paraffins, iso-paraffins, naphthenes, diolefins and aromarics
PP	Polypropylene
PS	Polystyrene
SEK	Swedish Krona
USD	United States Dollar

Contents

List of Figures

List of Tables

1

Introduction

1.1 Background

In Europe alone, 60 million tons of plastics were produced in 2018, of which only 25% of the collected plastic packaging was recycled, and the rest was incinerated or landfilled [4]. Increasing the fraction of plastics that are recycled is crucial to lower the fossil CO_2 emissions from combustion of municipal plastic waste. Today, the most preferred recycling technique is mechanical recycling, which involves reforming the waste into pellets without altering the chemical composition. The benefits with this method is that it is simple and has a low cost. However, it requires pure single-polymer streams which is difficult to obtain since plastic waste is a mixture of several different plastics. Mechanical recycling also deals with issues regarding quality of the polymer after each recycle step. This is due to crosslinking, branch formation and other chemical reactions that takes place during the extrusion process when recycling [5]. Because of these weaknesses, mechanical recycling is a very limited method for recycling plastic waste.

An alternative method is chemical recycling, which aims to break down the polymers into building blocks and then build up the polymers again. There are several chemical recycling methods, such as pyrolysis, hydrocracking and solvolysis. Pyrolysis is a promising technique to handle mixed plastic waste which cannot be recycled mechanically, such as multi-layer packaging and automotive shredder residues. The technique involves heating the waste to approximately $450°C$ in an inert atmosphere, which yields solid, liquid and gaseous products [6]. The solid product is mainly char, the liquids are waxes and pyrolysis oil and the non-condensable gases are among others CH_4, H_2, CO, CO_2, C_2H_4 and C_3H_6. The solid char is commonly separated using cyclones, and could further be used in various applications such as solid fuels or as activated carbon. The waxes, which become solid when cooled down to ambient temperature, are separated to not cause issues such as fouling in the process equipment. The gases are generally combusted and provides energy for the pyrolysis process, enabling it to be energy independent or even have a surplus of energy. In the context of chemical recycling of plastics, pyrolysis oil is the crucial component to separate in order to provide plastic production with raw materials [1].

The pyrolysis oil can be divided into different fractions of hydrocarbons depending on the number of carbon atoms in the molecules (carbon number) and the application of products with a specific range of carbon numbers. Different references have different definitions of what the different ranges of hydrocarbon numbers are named. In this project, the hydrocarbons with carbon numbers from C5 to C12 will be called naphtha [7], while the components from C13 to C19 will be called diesel [8]. The components lighter than C5 are called light gases or non-condensable gases, and waxes are defined as C20 or heavier components.

Today, building blocks for production of new polymers are produced from steam cracking of naphtha, which is mostly produced from fossil crude oil. The naphtha is heated up to 750-900°C, which cracks the naphtha into light olefins with free-radical mechanisms. The light olefins, such as ethylene and propylene, can after being separated be used as building blocks to produce polyolefins such as polyethylene (PE) and polypropylene (PP) [9]. If one can secure large quantity of naphtha fraction, the existing crackers could be used and thereby using existing equipment for producing thermochemically recycled plastics.

1.2 Aim

When performing pyrolysis of plastic waste, the separation of the pyrolysis products is complex due to a variable and partly unknown composition of the pyrolysis oil. Several separation techniques could be used, with different costs and performances. The types of polymers in plastic waste affects the pyrolysis products which in turn affects the separation process. Therefore the selected separation process must be robust and this master thesis has the following objectives:

- Evaluate different separation processes for pyrolysis products from plastic waste, in terms of performance and economics.
- Assess the performance of the separation process when varying the plastic waste feedstock, with the objective of evaluating its robustness and adaptability to feedstock variability.

1.3 Limitations

The project includes modeling of the separation between different oil and gas fractions, which is the "separation process" part in figure 1.1. This "separation process" will further be described in the method chapter. Before the separation process, there is a fluidized bed pyrolyis reactor with a cyclone to separated the solid char from the pyrolysis products. These will not be included in the simulations. After the separation process, the steam cracker and other pre-treatment steps of naphtha will not be included in the model either.

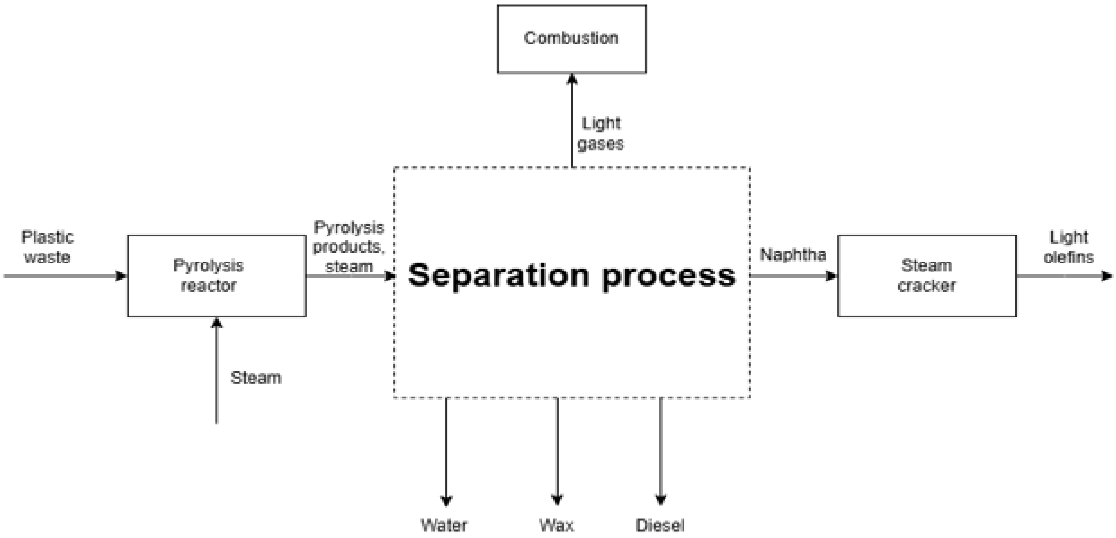

Figure 1.1: System boundaries for the separation process studied in this project.

Steam is assumed as fluidization medium in the pyrolysis reactor, therefore the results will be limited to that case and not for other fluidization mediums such as flue gases. Another limitation is that the plastics are assumed to be clean with no impurities such as biomass, food residue and heteroatoms such as sulfur, nitrogen and chloride. Further in the project, the only thing referred to as "impurities" will be water and unwanted molecules like acids. Pyrolysis products that are going to be considered are those coming from pyrolysis of PE, PP, polystyrene (PS) and polyethylene terephthalate (PET), since these plastics are the most common occurring in waste. Thereby, pyrolysis products from other plastics such as polyvinyl chloride (PVC) will not be considered. The pyrolysis product distribution from each plastic will be simplified in order to have a reasonable number of components in Aspen Plus. In practice, this means excluding fractions from the product gas that are very small or will be of little importance for the simulations. Also, some components that have similar properties (boiling point) will be modeled as one component. When modeling mixed plastic waste, experimental data will be used from individual plastics due to lack of data for mixtures. Therefore the data from that case can deviate from experimental results from mixed waste.

2

Theory

2.1 Plastic types

There are several types of plastics, of which many are present in municipal solid waste. PE has the most simple structure with single bonds between carbon and hydrogen atoms. It has various applications, such as for plastic bags and food wrapping. PP has similar structure as PE, but has a methyl group on every second carbon atom. Both PE and PP have problems with oxidation and chain scission, making them have a short lifetime when they are recycled mechanically [5]. Another reason for food packaging generating so much waste, where there is much of PE and PP, is that it has generally not been accepted using recycled plastic waste for food wrapping. This is because of the risk for contaminants from the recycling process ending up in the food. Therefore mostly virgin materials have been used for food wrapping, increasing the demand for fossil-based plastic. With new regulations though, there will be recycling chains that are accepted for producing new food wrapping from recycled plastic waste. These regulations will include different types of recycling, including chemical recycling which will be crucial to close the loop for plastic food packaging [10].

Another type that is common is PET which is widely used in beverage bottles due to its light weight, resistance to chemicals and that it can be recycled mechanically multiple times without loosing quality, unlike PE and PP. PET is also used in other food package applications, in textile industry, and in automotive and electronic applications [11]. Even if many beverage bottles that consist of PET are pre-sorted and recycled mechanically, there will still be a fraction that is mixed with other plastic waste that will be incinerated, or recycled in another way.

Lastly there is PS which is synthesized by styrene monomers, and has mainly applications for protective packaging such as insulation and where the visibility is important like display items and clear containers. It is also used in toys and other household products [12].

Since plastic waste often comes as a mixed stream of different plastics, there needs to be a way to define such mixture of plastics. In European facilities, packaging types are defined according to the Deutsche Kunststoff Recycling (DKR), for setting minimum quality standards. One such defined mixture of plastics is DKR-350, which is the mixture that is remaining when all the easy reusable plastics have been sorted out. DKR-350 has low recycling value, since it has high variability in properties and is sometimes highly contaminated. The major components in DKR-350 are PE and PP, which constitutes about 50% of the weight. Next comes PET with 20 wt%, followed by PS with 3.4 wt%. The rest of the share in DKR-350 consist of clogged materials, multilayer flexibles and other plastics [13].

When plastic waste is pyrolyzed, the condensable gases that yield the pyrolysis oil consist of many different hydrocarbons. Which hydrocarbons that are formed depend on different parameters such as retention time and temperature but also which plastics that are in the plastic mix. As an example, PP yields a high amount of isoolefins, while the oil of PE has more n-paraffins. The reason for this has to do with the structure of the polymers, with PP having a branch every second carbon atom the pyrolysis products from PP will of course be more branched. One effect of this is for example that product streams from PE compared to PP requires less processing before later process steps such as steam cracking. Apart from the differences in branching and double-bonds, a difference between plastic types is the number of carbon atoms in the molecules of the pyrolysis oil. All plastics give a large variety of hydrocarbons of different molecular sizes, but for example plastics rich in PP have a wider range of carbon numbers than PE [4]. The product gases differences in saturation, branching, carbon number and if they are aliphatic or aromatic affect their boiling point, which affects the dimensioning of a separation process.

2.2 Separation methods for condensable products

When separating the gaseous components from the condensable, there are three main methods that uses different separation equipment. One method is to cool the stream down with a heat exchanger to have a mixture of vapor and liquid, and then separate the two phases by gravity with a flash tank. There are vertical and horizontal versions of this separation equipment but in this project, the focus will be on the vertical types. The flash tank can be divided into different sections, where the inlet section usually has some equipment in the form of a cyclone and guide plate. The second section is the settling section where the separation between gas and liquid droplets occur, and this is where the key parameters are found for the dimensioning of the equipment. The final section is the defogging section, or the demister pad, that consist of a mesh to catch small droplets from the gas before the gas outlet. The benefits with a flash tank is that it is a simple type of equipment that can handle large flows, has low pressure drop and is easy to control. On the other hand, the separation between liquid and vapor is bulky since it only can handle large liquid drops, up to around 100 μm [14]. A drawback is also that having a cooler, the sudden temperature drop of the stream causes that all condensable products do not fully condense, which gives a lower yield of pyrolysis oil [1].

Another alternative is using distillation for separating fractions in a mixture with different boiling points, which uses the equilibrium-diffusion principle. The components with lower boiling points are more volatile and evaporate first, while the heavier components remain liquid. Through repeated vaporization and condensation, two streams are obtained with light and heavy components respectively. There are several benefits with distillation, among others high heat and mass transfer rates and high thermodynamic efficiency [15]. A drawback though with distillation columns compared to using a condenser and flash tank is that it is a more energy demanding process due to that the bottom product usually is reboiled and circulated back to the column. This causes the distillation column to have higher operating costs than flash tanks [1]. Also when considering capital costs, distillation columns is usually the more expensive alternative due to the more complex design, the cost for trays or packing material and the larger size if there is reflux. Distillation columns can also be more difficult to size correctly if the composition of the stream to the columns is unknown, which can be the case for pyrolysis products from mixed plastic waste. Figure 2.1 shows how both a condenser with flash tank and a distillation column can be used in a process for separation pyrolysis oil from non-condensable gases.

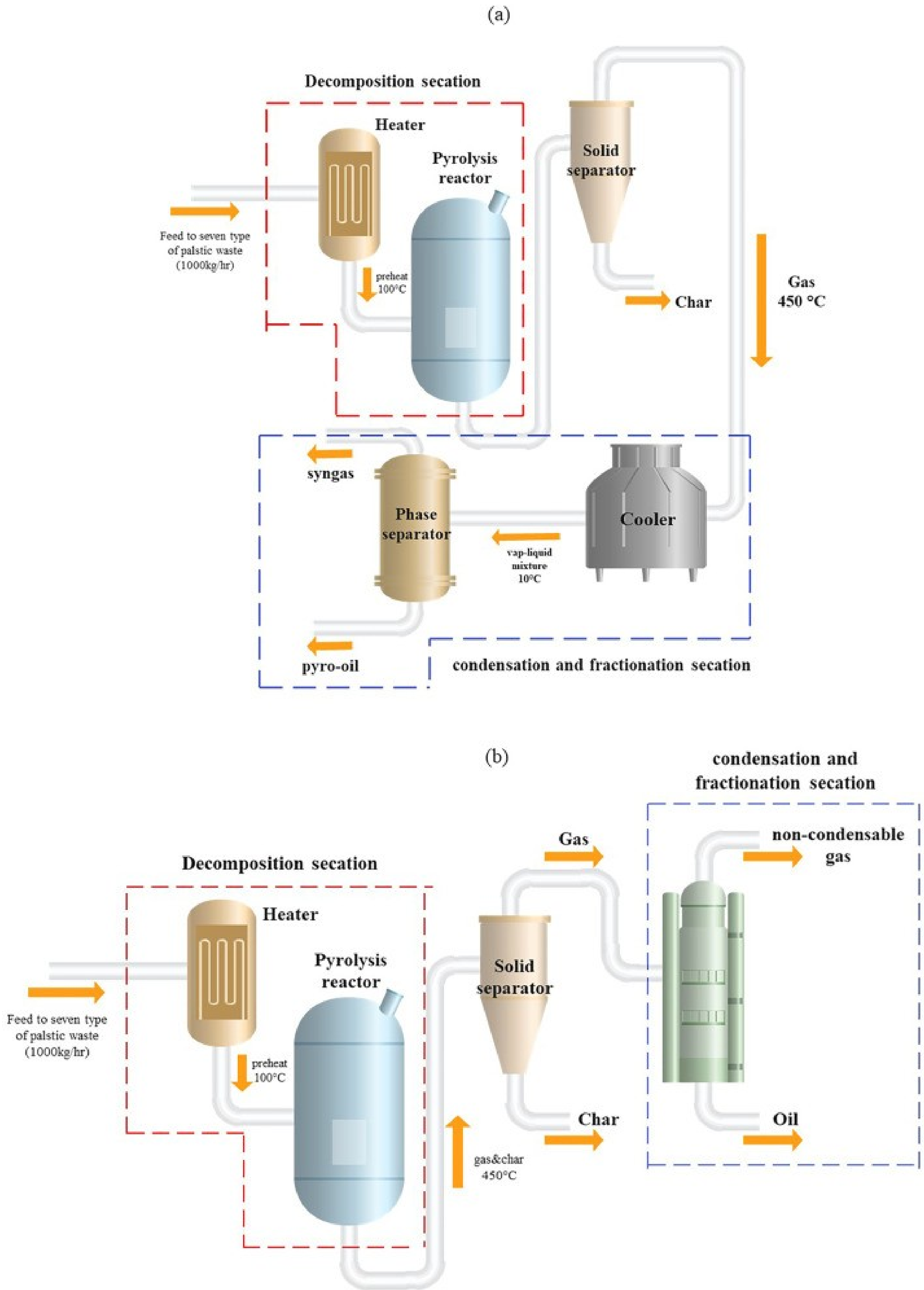

Figure 2.1: Separation of pyrolysis products using a) cooler and flash tank b) distillation column [1].

The third separation technique is to use a spray column followed by tube and shell heat exchangers, which has been investigated for separation of condensable products from pyrolysis of biomass. In that case, pyrolysis oil is re-circulated through a heat exchanger before entering the spray column to quench the volatile vapors. The benefit with this separation method is that it is good for collecting aerosols from the vapor, but the direct contact between the hot vapors and the pyrolysis spray can cause reactions in the spray which will eventually lower the liquid yield [2]. Another weakness is that since it is difficult to control the temperature of this type of process, it is diffidult to get the exact fractions of the pyrolysis oil that are desired [16]. Figure 2.2 shows the principle of using a spray column with recirculation of pyrolysis oil.

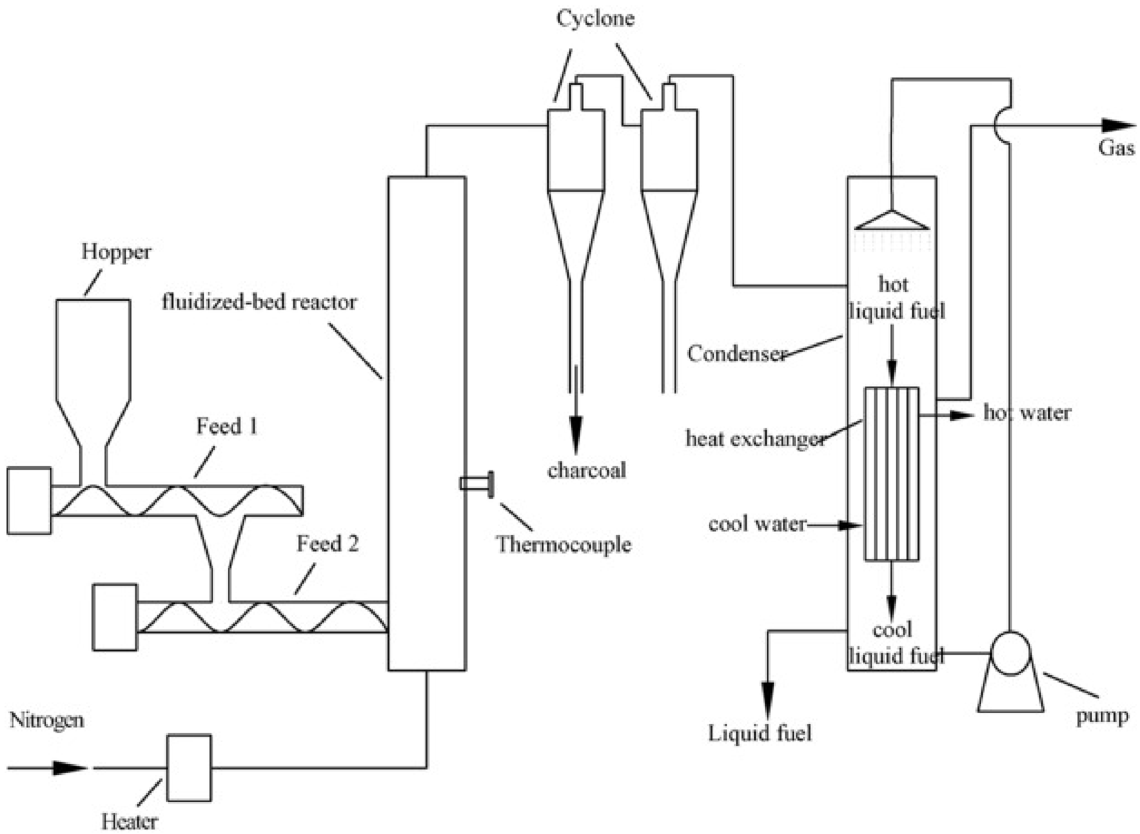

Figure 2.2: Separation of pyrolysis products using a spray column [2].

All of these three processes are relevant for separating different fractions of the pyrolysis oil and the non-condensable gases. A distillation column is the method that has the most exact separation between hydrocarbons of different boiling points, so that will be the method used when needing the highest purity. For streams with lower requirements of purity, heat exchangers with flash thanks and spray columns are two alternatives. As stated before, it is easier to control the temperature in heat exchangers than in spray columns. Therefore, heat exchangers with a following flash tank will be the main separation units used when a fraction with less requirements on purity need to be separated.

2.3 Fluidization medium

2.3.1 Choise of fluidization gas

There are different gases that can be used as fluidization gases for pyrolysis of plastic waste. Some common examples are steam, nitrogen or recirculated pyrolysis gases [17]. A benefit with steam is that it is easy to separate from the pyrolysis products after the fluidization, which is easily done with coolers and flash tanks. Another benefit is that it is cheap compared to nitrogen, and it reduces the formation of soot. Recirculated product gases on the other hand, will increase the residence time in the fluidized bed zone which can cause unwanted secondary reactions that form more aromatics and coke. Therefore, steam was chosen as a fluidization medium for this process. A drawback with steam though is that it is energy demanding to produce.

2.3.2 Fluidization gas mass flow rate

A proper ratio between the plastic feedstock mass flow and the fluidization gas mass flow needed to be chosen, in order to have a realistic steam mass flow in the separation process. A small steam mass flow is preferred in the separation process to reduce the equipment size, but it has to be large enough to give a proper fluidization velocity in the pyrolysis reactor. Lee et al. performed experiments on a fluidized bed reactor where they varied the fluidization gas flow between 0.75 and 1.5 L/min, and the plastic feed was varied between 0.5 and 0.7 g/min, with temperatures from 550°C to 650°C [18]. Assuming the fluidization gas as an ideal gas, a mass flow could be calculated and from that a ratio between the fluidization gas mass flow and the fuel mass flow. With 1.5 L/min fluidization gas, 0.5 g/min plastic feed mass flow and a temperature of 550°C the ratio between the fluidization gas and the plastic feed was 0.78, which is the ratio that is used further when doing simulations.

2.4 Software

For this project, two softwares were used apart from Microsoft's Office package.

2.4.1 Aspen Plus

Aspen Plus is the leading process simulation software in the chemical industry. It has capability to handle a large range of chemical processes, including hydrocarbon distillation which is most relevant in this project. To it's help, it has a built-in physical properties database for a large variety of compounds. Many different process equipments such as heat exchangers and distillation columns can be used and connected with streams, to simulate different processes [19]. This is the main software that is used when simulating the processes in this project, with each separation step.

2.4.2 Aspen Energy Analyzer

Aspen Energy Analyzer is another software from Aspentech that is used to analyze potential energy saving in chemical processes. It can create heat exchanger networks, as well as hot and cold composite curves and grand composite curves (GCC) to analyze the best solutions for energy recovery [20]. This software is not used as much as Aspen Plus in this project, but is a tool to generate GCCs in order to see if the process is self-sufficient in terms of energy. It is also used for determining the amount of utilities needed in the processes, and their cost.

3

Methods

This chapter describes the methodology for the project, when defining the pyrolysis product distributions, designing and simulating the process in Aspen Plus and performing the sizing and economic assessment. Three different processes are described, with varying level of complexity. A smaller energy analysis was performed for process 3 and finally the sizing and economic evaluation are described which was performed for all processes.

3.1 Pyrolysis product compositions

3.1.1 Polyethylene

To determine the composition of the pyrolysis gases that are fed to the process, data from various literature was used. To start with, data from a quantitative two-dimensional gas chromatography (GC) analysis in [21] (figure 3) was used to determine the distribution between different carbon numbers in the pyrolysis oil. The figure provides a clear distribution between the carbon numbers from 5 to 40, and for each carbon number it shows the distribution between α-olefins, iso-olefins and PINA (n-paraffins, iso-paraffins, naphthenes, diolefins and aromatics). However, the PINA distribution is also important to know, so for that data was used from [4] (figure 6). The two sources have data for HDPE and PE films respectively, but in this project no distinction between the those two types of PE was made and the data was therefore combined. The PINA distribution was assumed to be equal for each carbon number, except for the aromatics. For those, it was assumed that all aromatics were equally distributed between carbon number 6 (benzene), 7 (toluene) and 8 (m-xylene and styrene). Apart from the pyrolysis oil, a distribution of the light gases needed to be defined. Williams and Williams performed experimental pyrolysis on PE for different temperatures, of which the lowest was 500°C [22]. The temperature was considered to be close enough 450°C, which is the pyrolysis temperature in this work, to use their gas distribution results from GC analysis. With the data from these sources combined, a full distribution between the different components from carbon number 1 to 40 could be created. However, it was not necessary to have a so exact distribution for all carbon numbers since it is mainly naphtha that needs an exact separation and for example the composition of the waxes was not as important. Also, to have more components as an input in Aspen Plus would require more time and would increase the computational time. Therefore, the distribution was simplified to not include every component for the higher carbon numbers. From carbon number 13 to 20, every second carbon number was defined and for the ones higher, every 10th carbon number. All components were modeled as n-paraffins for those heavy molecules to simplify even more, and the differences in molecular structure were assumed to not have such a big impact (e.g. boiling point) for the heavier molecules as for the lighter. The resulting component distribution can be viewed in table 3.1.

Table 3.1: Weight-% of components from PE pyrolysis. Carbon number 0 is hydrogen.

Carbon Number	Alpha-Olefins	Iso-Olefins	n-Paraffins	Iso-Paraffins	Di-olefins	Naph-thenes	Aro-matics
0			1.05				
1			0.83				
2	2.19		0.78				
3	1.82		0.76				
4	1.89	1.02	0.42	0.08			
5	0.53	0.00	0.40	0.08	0.05	0.14	
6	2.05	0.09	0.30	0.06	0.04	0.10	1.12
7	1.16	0.00	1.21	0.23	0.15	0.41	1.12
8	1.16	0.27	1.41	0.27	0.18	0.48	1.12
9	1.25	0.18	1.26	0.24	0.16	0.43	
10	1.34	2.41	1.16	0.22	0.15	0.39	
11	1.25	0.27	1.01	0.19	0.13	0.34	
12	1.16	0.45	1.26	0.24	0.16	0.43	
13	2.41	1.07	2.27	0.43	0.28	0.77	
15	8.20						
17	4.37						
20	26.12						
30	7.49						
40	0.89						

3.1.2 Polypropylene

The composition of the pyrolysis products from PP was determined in a similar way as PE. Figure 3 in [21] provides a distribution between the carbon numbers for PP pyrolysis oil, apart from PE. For the PINA distribution, PP rigids in figure 6 in [4] was used. To know the fraction between light gases and pyrolysis oil, figure 2 in [23] (slow atm, 450°C) was used, which shows the weight percentages of heavy oil, light oil, gases and char. Since char is assumed to be separated prior to the simulation of this process, that fraction was not taken into account. The data was therefore normalized to just show the distribution between gases and oil, which were 6.4 and 93.6 wt% respectively. For the distribution between the components of the light gases, two sources were combined. Figure 4 in [24] shows distribution between the gases up to C3, including hydrogen, but not the C4 gases. Meanwhile, figure 6 in

[23] (slow atm, 450°C) has the distribution between carbon number 1 to 5, but not hydrogen. The important was to find a distribution between C1 to C4 and hydrogen, so the two datasets were combined to give a complete composition of the light gases. The only missing data was the distribution between different components of C4, so therefore they were assumed to be evenly distributed between α-olefins, iso-olefins, n-paraffins and iso-paraffins. The data was then compiled into a table where it was simplified in the same way as for PE, and is shown in table 3.2.

Table 3.2: Weight-% of components from PP pyrolysis. Carbon number 0 is hydrogen.

Carbon Number	Alpha-Olefins	Iso-Olefins	n-Paraffins	Iso-Paraffins	Di-olefins	Naph-thenes	Aro-matics
0			0.67				
1			0.37				
2	0.00		0.28				
3	4.31		0.00				
4	0.18	0.18	0.18	0.18			
5	0.00	0.19	0.05	0.07	0.29	0.04	
6	0.00	5.99	0.19	0.30	1.23	0.19	0.29
7	0.00	1.50	0.09	0.14	0.58	0.09	0.29
8	0.00	2.81	0.16	0.24	0.99	0.15	0.29
9	0.09	16.11	0.14	0.21	0.88	0.13	
10	0.00	3.65	0.09	0.14	0.58	0.09	
11	0.09	0.56	0.06	0.10	0.41	0.06	
12	0.00	3.09	0.06	0.10	0.41	0.06	
13	0.09	0.66	0.11	0.17	0.70	0.11	
15	8.58						
17	3.02						
20	4.44						
30	15.00						
40	17.27						

3.1.3 Polystyrene

The pyrolysis products for polystyrene were determined in a different way. For this plastic the largest share of the product gases consist of aromatics, and they have not such high carbon numbers as for PE and PP. Zayoud et al. performed pyrolysis in a pilot-scale reactor, with 450°C and 1 bar as operating conditions, and analyzed the products with two-dimensional GC [25] (table 1). The results show a distribution between various mono-, di- and triaromatics. However, there are fractions with for example "other monoaromatics" and light gases which needed to be determined. For the light gases, data from Lian et al. was used where they analyze the pyrolysis products from pyrolysis of PS at 460°C [24] (figure 4). The gas analysis only shows the gases up to C3 though, so to determine the amount of C4 data was used from

Royuela et al. where they analyze gases from pyrolysis of PS in an auger reactor, with a temperature of 450°C and a feed rate of 9 kg/h [26] (table 2). Finally to know the components of the C4 gases, data from Park et al. was used, where they perform two-stage pyrolysis of PS [27] (table 3). The last source is not at the same conditions as this project, but however it covers the composition of C4 gases which are not covered in detail by the other sources. The data from Park et al. was also used to determine the distribution between the minor components of the mono-, di- and triaromatics, as well as for the aliphatics. The final distribution between the products from pyrolysis of PS is shown in table 3.3. When studying the table, it can be seen that the mixture is largely dominated by styrene and ethylbenzene, while the light gases only represent a very small fraction.

Table 3.3: Weight-% of components from PS pyrolysis.

Gases	**wt-%**
Hydrogen	0.037
Methane	0.268
Ethane	0.167
Ethylene	0.344
Propylene	0.047
1-Butene	0.071
1,3-Butadiene	0.008
Higher Aliphatics	**wt-%**
1,3-Cyclopentadiene	7.529
Monoaromatics	**wt-%**
Benzene	0.280
Toluene	5.765
Ethylbenzene	13.882
Styrene	42.000
Cumene	0.700
Alpha-Methylstyrene	7.176
Propenylbenzene	0.560
Indene	1.049
Diaromatics	**wt-%**
Stilbene	2.225
1,3-Diphenylpropane	5.059
1,3-Diphenylpropene	1.059
2,4-Diphenyl-1-butene	1.529
1,4-Diphenyl-1,3-Butadiene	4.963
Naphthalene	0.342
Triaromatics	**wt-%**
2,4,6-Triphenyl-1-Hexene	2.824
Phenylnaphthalene	2.118

3.1.4 Polyethylene terephthalate

The distribution between the products from pyrolysis of PET were determined from experimental data provided by Dhahak et al [28]. The experimental setup was a tubular reactor, where the feed was heated up to different temperatures, but for this project the relevant temperature was 450°C. Different analytical methods were used to determine the composition of the gaseous and waxy products, such as GC and mass spectroscopy. Figure 9 was used to determine the ratio between gaseous and waxy products, while figures 13 and 15 were used for the composition of the gas and wax respectively. The analytical methods could not detect all the components though, but the most abundant were quantified and are shown in table 3.4.

Table 3.4: Weight-% of components from PET pyrolysis.

Gaseous products	**wt%**
Acetaldehyde	13.962
Carbon dioxide	12.152
Carbon monoxide	5.688
Ethylene	0.427
Benzene	0.271
Waxy products	**wt%**
Benzoic acid	39.760
Monovinyl terephthalate	9.175
4-methylbenzoic acid	3.823
4-ethylbenzoic acid	3.058
4-vinylbenzoic acid	2.447
Biphenyl-4-carboxylic acid	0.918
Monoethyl terephthalate	1.285
Divenyl terephthalate	0.734
1,2-ethanediol dibenzoate	0.612
Biphenyl	4.282
Terphenyl	1.407

3.1.5 Mixed plastics

To simulate a stream of mixed waste plastics, the mixture DKR-350 was used. It is a mixture of different plastics that remains after the easy reusable plastics have been sorted out, and is the largest post-consumer plastic packaging waste stream in Europe. The mixture contains the four plastics that have been discussed previously, as well as clogged materials and multilayer flexibles. The PE and PP are also divided into rigids and films [29]. For simplicity, the clogged materials and multilayer flexibles were neglected in this work and there was no distiction between rigids and films. The resulting distribution between the four plastics in DKR-350 is shown in table 3.5.

Table 3.5: Weight-% of plastics in DKR-350 mixture.

Plastic	wt%
PE	48.3
PP	19.3
PS	4.70
PET	27.7

When a stream of mixed plastic waste such as DKR-350 is being pyrolyzed, reactions occur between the pyrolysis products of the different plastics. The pyrolysis products of mixed plastic waste will therefore not be the same as for the individual plastics combined. The composition of the pyrolysis product stream is difficult to predict, due to the reactions between the components. Genuino et al. performed pyrolysis experiment on individual plastics as well as DKR-350, and constructed a linear model for the individual plastics to predict the pyrolysis products from DKR-350. The model was then compared with the actual products from DKR-350, to see how large the difference was between the model and the experiment. The results showed that pyrolysis of PET yields a large fraction of solid residues, which interacts with the polyolefins giving a lower yield of oil and wax. However in this project, the solid residues are assumed to be pre-separated before entering the process that is modeled, and it is mainly the composition itself of the wax, oil and gas that is interesting. The results also showed that the predictability of the aliphatic compounds was very good, with a deviation of maximum 6% between the linear model and the experimental results. The amount of aromatic components was however not so easy to predict, which most likely depend on the interaction between PET and polyolefins that form solid residues, which lower the aromatic yield [29]. With these results, it can be supported that the simulations in this project can be performed without taking the reactions between the different plastics into considerations, and still trust the composition of the aliphatic components. The aromatic components will most likely be less in reality than in the model though, which will be discussed.

3.2 Process descriptions

Three different processes were modeled, to compare their costs and performances. Process 1 in figure 3.1 is the simplest process, that only separates away the most essential components to obtain pyrolysis oil. This is used by having heat exchangers that partially condense the mixture of pyrolysis products and steam, with following flash tanks that separate the liquid and vapor phases. Process 2 in figure 3.2 is slightly more advanced, with one extra heat exchanger and flash tank so that the pyrolysis oil is separated into the diesel and naphtha fractions. Finally figure 3.3 show process 3. This process has more advanced separation of naphtha and diesel, with distillation columns instead of flash tanks. All the components in the flow-sheets are numbered, and will be referred to further in the text with bold text and parenthesis **(like this)**.

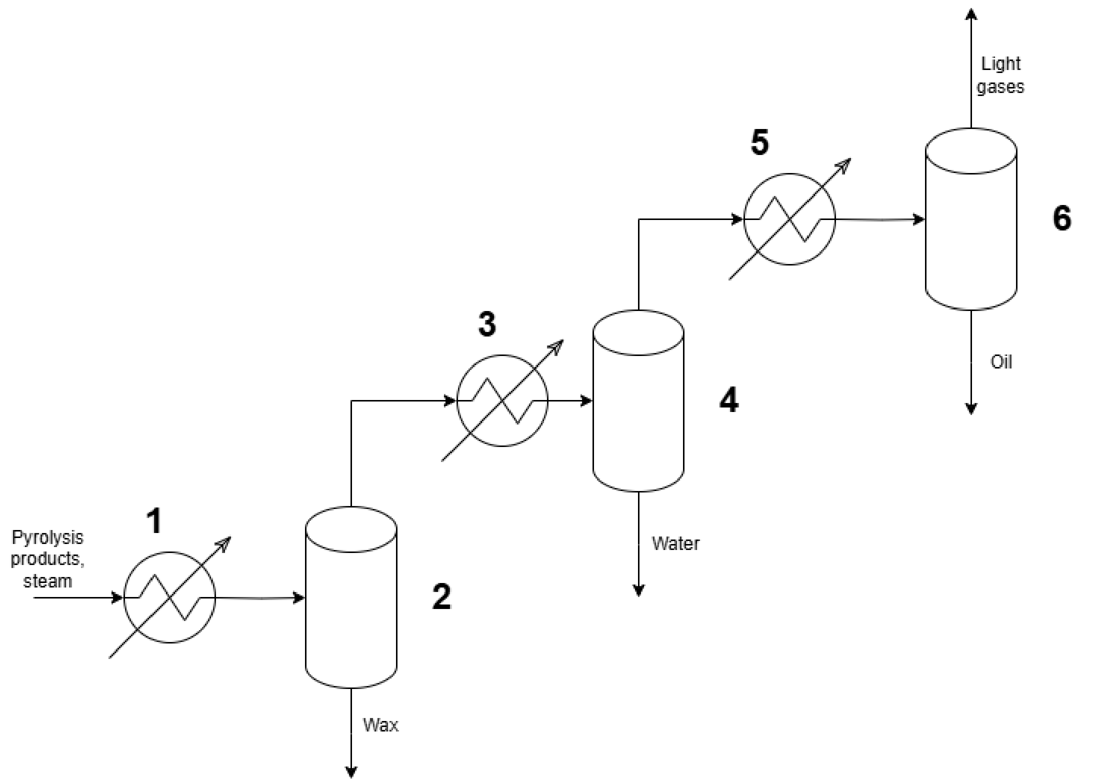

Figure 3.1: Flowsheet of process 1.

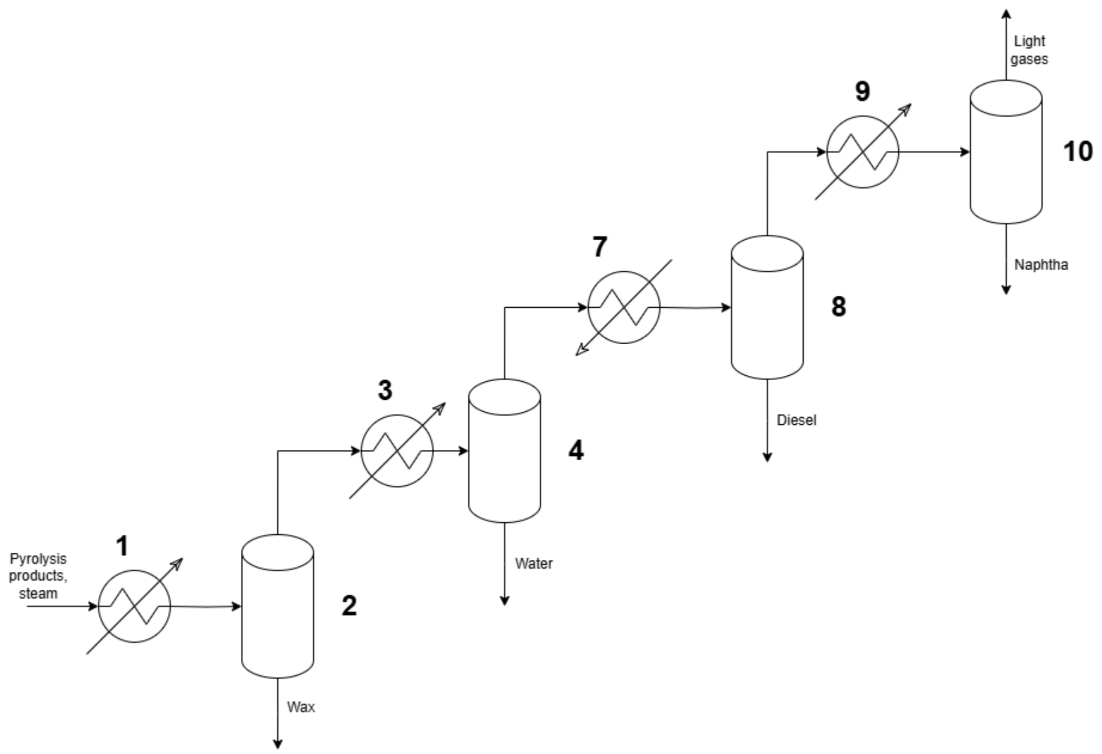

Figure 3.2: Flowsheet of process 2.

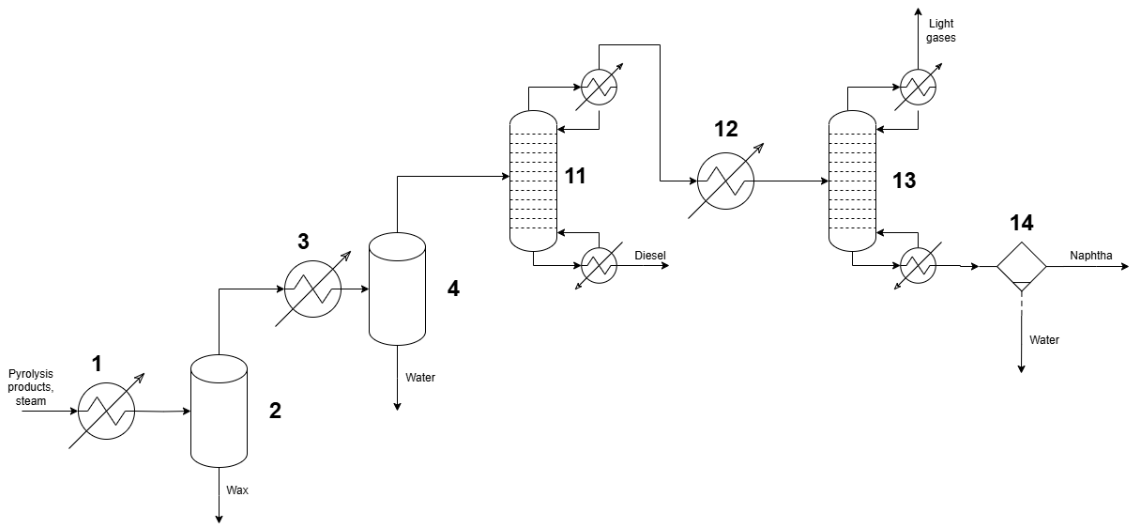

Figure 3.3: Flowsheet of process 3.

3.3 Setting up the simulation

All the pyrolysis products that are in tables 3.1, 3.2, 3.3 and 3.4 were added to the Aspen Plus simulation files. Some replacements of components needed to be done though since not all components were available, mostly for PET. For example, mono- and divinyl terephthalate were replaced with terphthalic acid and 4-ethyl- and 4-vinylbenzoic acid were replaced with 4-methylbenzoic acid. In general though, the pyrolysis products found in literature were found in the Aspen Plus database and if not, similar components were used. Four different streams were created where each stream had the composition of the pyrolysis products from each plastic respectively. A selector was then inserted, so that different plastic waste streams could be chosen depending on which one that was going to used for different modeling cases.

Peng-Robinson's equation of state was used for the simulations in Aspen Plus, because it is preferred for simulations with hydrocarbon mixtures which are non-polar. It is also the most commonly used method when simulating crude oil distillation, which is rather similar to the types of simulations in this project [30]. A limitation with Peng-Robinson's equation of state is though that it only models vapor-liquid equilibrium, and not the transition between liquid and solid phases. Therefore there can be some uncertainties when modeling waxes, at which temperatures they solidify.

For the feed, a mass flow of 2500 kg/h of pyrolysis products was simulated, which corresponds to roughly 20 kton/year. On top of this, a steam mass flow was added for the fluidization medium. The amount of steam was 78% of the pyrolysis product mass flow, according to the literature study.

3.4 Separation steps

3.4.1 Separation of waxes

The first step in the separation process was to separate the waxes from the rest of the hydrocarbons. The separation of waxes was good as a first separation step, since they otherwise can become solid at lower temperatures downstream in the process and can cause problems in equipment. Also, since the stream that comes directly from the pyrolysis reactor was hot (450°C) it was more energy efficient to separate the waxes first, before separating components with lower boiling points such as water. The separation was not necessary to be very exact between two carbon numbers because neither the waxes or the diesel was a product that needed high purity for this scope. Therefore, a cooler **(1)** and a flash tank **(2)** were sufficient to obtain a separation that was good enough. Which purity that was "good enough" was arbitrary, and was a trade off between having more light hydrocarbons in the liquid phase or having more of the heavy hydrocarbons in the vapor phase. The amount of light and heavy components in each separated phase depended on the temperature and pressure, however changing the pressure would increase the cost of the equipment and was not considered necessary in this separation step. Therefore, only the temperature was varied in order to alter the compositions of the liquid and vapor phases. Figure 3.4 shows the relation between the mass fractions of n-eicosane, n-heptadecane and n-pentadecane in the vapor phase and the temperature in the flash tank. The component n-eicosane has carbon number 20 and was used to represent the lightest waxes, while n-heptadecane and n-pentadecane have carbon numbers 17 and 15 respectively, and represented the heaviest oil components. Ideally, n-eicosane should be completely in the liquid phase and n-heptadecane completely in the vapor phase to get a complete separation of wax without sacrificing too much of the oil components, but that would require a more advanced separation technique than a flash tank.

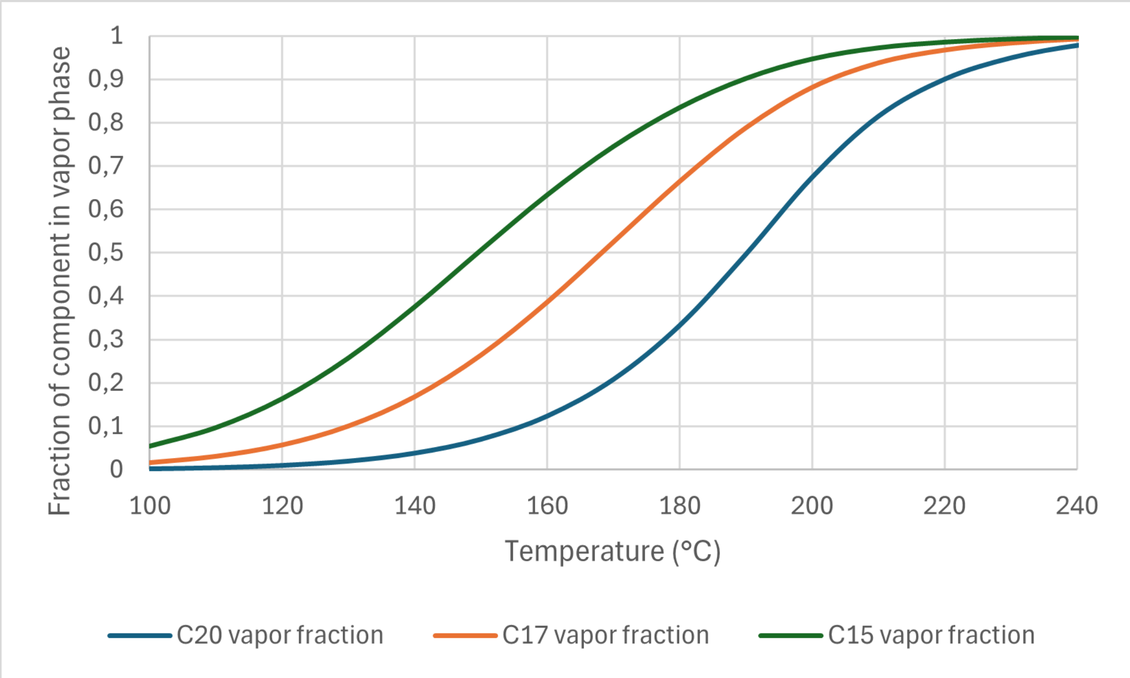

Figure 3.4: Mole fraction of n-eicosane (C20), n-heptadecane (C17) and n-pentadecane (C15) in feed to flash that end up in vapor phase, depending on temperature.

3.4.2 Separation of water

Water was a crucial component to separate early in the separation process in order to reduce the mass flows downstream. The water comes mainly from the fluidization medium which is steam, but minor parts could come from contamination of the plastic waste. To separate the water, a second cooler **(3)** with a flash tank **(4)** was used. Figure 3.5 shows the fraction of water that ends up in the liquid phase depending on temperature. In the figure it can be seen that when going below 95°C the concentration of water in the liquid phase increases rapidly.

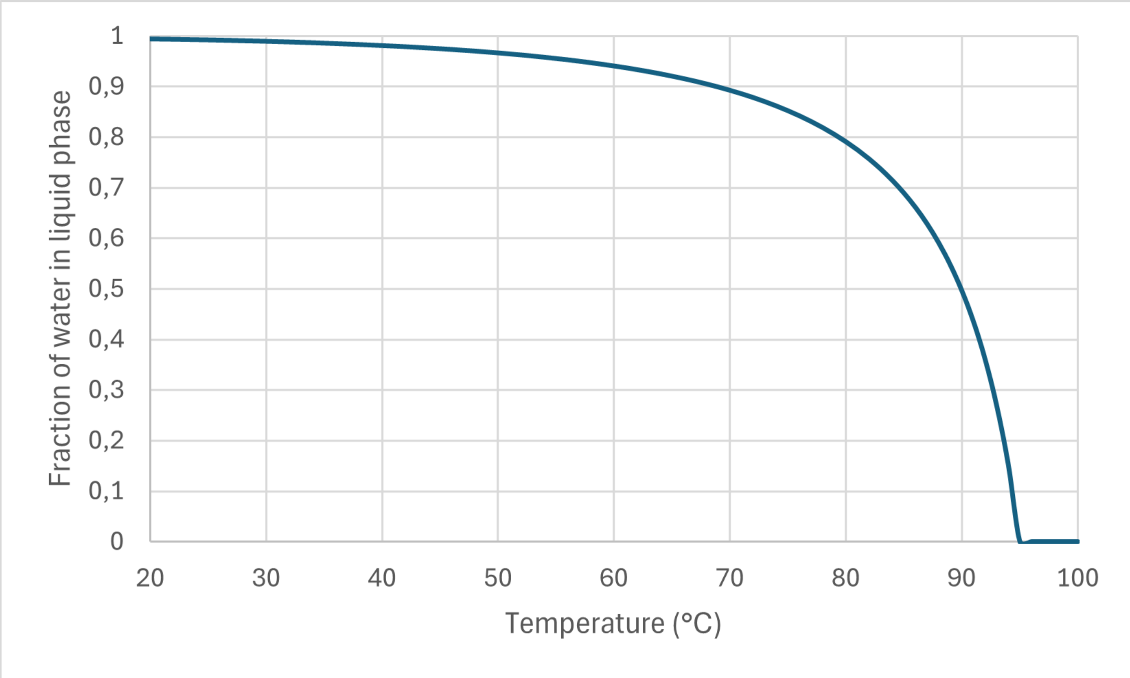

Figure 3.5: Mass fraction of water in feed to flash that end up in liquid phase, depending on temperature.

3.4.3 Separation of oil

After the separation of waxes and water, process 1 had only separation between pyrolysis oil and light gases, with no distinction between the fractions of the pyrolysis oil. As the previous separation steps, a cooler **(5)** and flash tank **(6)** were used.

3.4.4 Separation of diesel

3.4.4.1 Flash tank

Process 2 had a separation between diesel and naphtha, unlike process 1. This was done by having an additional heat exchanger and flash tank. After the separation of water, a heater **(7)** raised the temperature, to evaporate most of the components in the naphtha and light gases. A flash tank **(8)** then separated the diesel.

3.4.4.2 Distillation column

Process 3 had a more advanced separation process for separating the diesel fraction, a distillation column **(11)**. The column focused on separating the diesel and naphtha, a cut between C12 and C13. Before the stream went into the distillation column though, the hydrogen was separated from the rest of the components. This was because the hydrogen, which is very volatile, would influence the vapor-liquid equilibrium calculations in a way that was not consistent with a real process. In reality though, the separation would not exist and the hydrogen would follow with the rest of the stream in the distillation columns. Therefore, the separation of hydrogen was not included in the flowsheet.

To get an initial guess for different parameters in the distillation column such as reflux ratio and number of stages, a DSTWU column was used in Aspen Plus. This type of column uses shortcut calculations that has various assumptions, and therefore the results were not very accurate. It was still useful though, because it converged easy and gave a relationship between the number of stages and reflux ratio, so that a starting guess was provided for the rigorous distillation column. The light and heavy keys were specified as n-dodecane and n-tridecane respectively, which represent the cut between C12 and C13. The recovery of the light and heavy keys in the distillate were set to 95% and 5% respectively. A very large reflux ratio was set first, just to get the column to converge. Figure 3.6 shows the resulting curve that describes the relation between reflux ratio and number of stages. In general, increased number of stages increases the capital cost while an increased reflux ratio increases the operating cost. Therefore, a good choice for the number of stages is before the curve becomes flat. After setting the number of stages, parameters such as reflux ratio, feed stage and distillate to feed fraction could be determined which were used as initial input data in the rigorous distillation column.

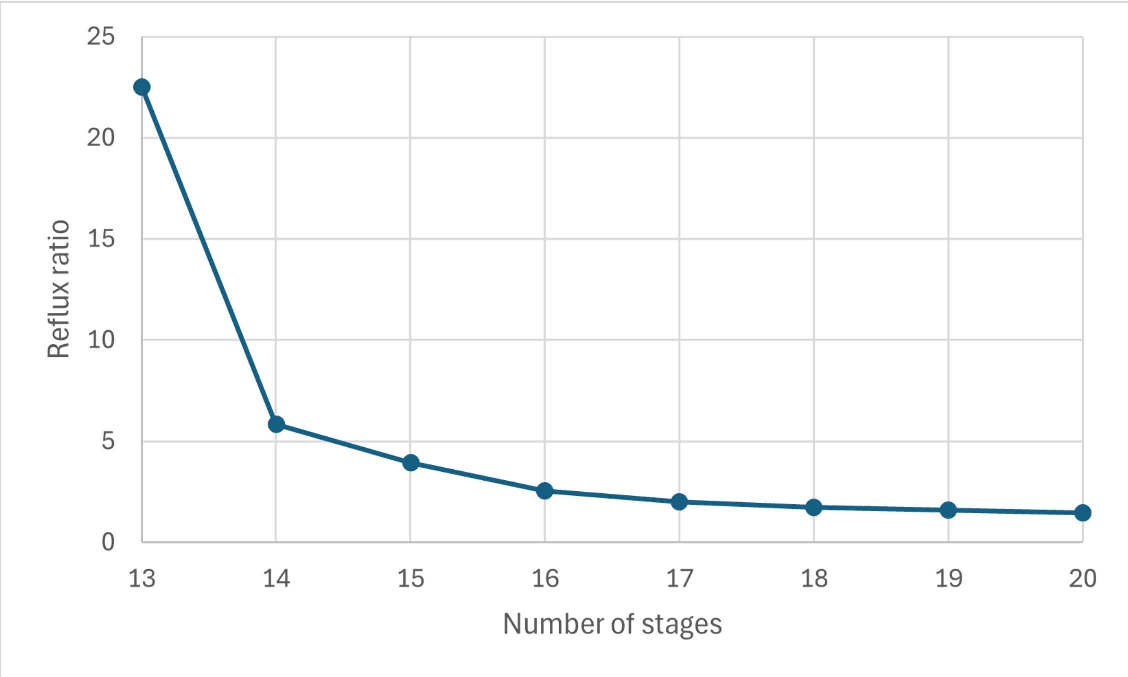

Figure 3.6: Reflux ratio depending on number of stages in distillation column 1.

As a rigorous distillation column, RadFrac was used in Aspen Plus. The stream that was fed to the distillation column was duplicated so that there was a parallel stream with a RadFrac column instead of DSTWU. The data from the shortcut column was used as initial data, but in order to optimize the column in the context of energy consumption the sensitivity analysis tool in Aspen Plus was used. What determines the energy consumption is mainly the boilup ratio, so in that aspect the boilup ratio should be as low as possible. However, the lower boilup ratio also means a worse separation. In this column, a limit of 95% recovery of both the light and heavy key was set to ensure that the product still had good quality. Different reflux ratios were tested, and for each reflux ratio a sensitivity analysis for different boilup ratios were performed. If the boilup ratio was too low, too much of the light key ended up in the bottom and vice versa. Figure 3.7 shows the mole fractions of the light key in the bottom product and the heavy key in the top product, and how they vary depending on boilup ratio.

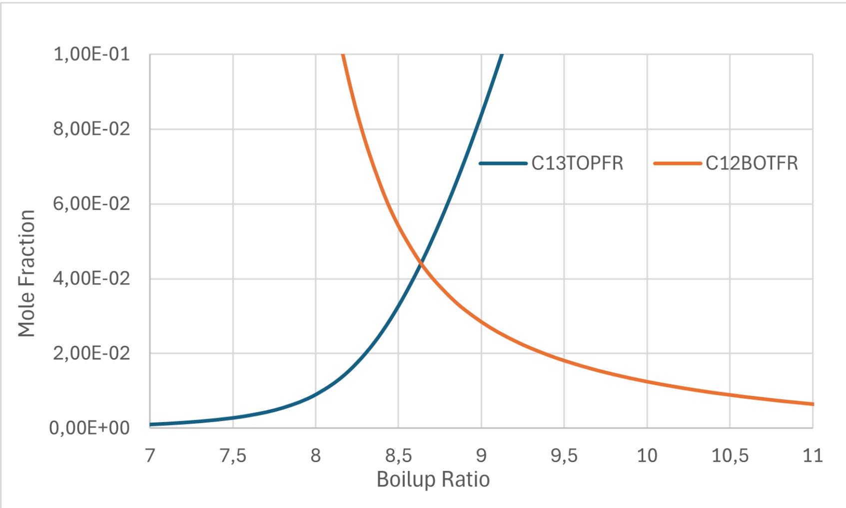

Figure 3.7: Fraction of n-dodecane (C12) that end up in bottom product and fraction of n-tridecane (C13) that end up in top product, when RR=0.2 and BR is varied.

3.4.5 Separation of naphtha

3.4.5.1 Flash tank

Process 2 had a simple separation between the naphtha and light gases, after the separation of diesel. One additional cooler **(9)** lowered the temperature, and a flash tank **(10)** separated the liquid phase and vapor phase respectively.

3.4.5.2 Distillation column

After the first distillation column in process 3, the hydrocarbons heavier than C12 had been separated away. However, there still needed to be a separation between C4 and C5 to obtain a rather clean naphtha stream. The components lower than C5 have a boiling point below room temperature, so they would stay as gases when the streams had cooled down after the separation. To have a good separation between C4 and C5, an atmospheric column was not enough since the light hydrocarbons would not condense at temperatures which were not extremely low. Different pressures were tested for the second column **(13)**, to see at which pressure there could be a proper separation between C4 and C5. For each pressure tested, the same procedure was followed as for the first distillation column, with first using the DSTWU column to get an initial guess for the number of stages, feed stage, reflux ratio and boilup ratio. As in the first column, a 95% separation of the light and heavy keys respectively were specified. The data from the DSTWU column was used in the

RadFrac column, and the reflux and boilup ratios were varied. Regarding the feed to the column, the vapor fraction needed to be adjusted so that the stages did not dry up. For all cases the vapor fraction was set to 0.6, except for 15 bar where it had to be lowered to 0.1.

Table 3.6 shows some of the configurations tested, with pressure, reflux and boilup ratios, the fraction of C4 in the top product, the fraction of C5 in the bottom product and the condenser temperature. For the cases of 1 bar, there was no configuration that gave good separation for both the light and heavy key. Since it was more important to obtain a clean naphtha stream rather than have a clean gas product, a constraint was set to separate at least 95% of C4 to the distillate. If more C4 was in the top product, there was less of C5 in the bottom and therefore the reflux and boilup ratios that gave 95% separation of C4 were chosen. For higher reflux ratios, the boilup ratios needed to be higher as well to not get an extremely low condenser temperature. This resulted in higher separation of C4, but lower separation of C5.

When increasing the pressure to 5 bar, the separation seemed to be about the same as for 1 bar. The difference was that higher boilup ratios were required, which resulted in higher condenser temperatures. For higher reflux ratios such as 1.5, the condenser temperature gets very low. The lowest acceptable condenser temperature was then set to 25°C to be able to use normal cooling water as utility. When further increasing the pressure to 10 bar, there was no significant difference compared to 5 bar. At 15 bar though, a very pure separation of both the light and heavy keys could be obtained for temperatures which were above 25°C. When plotting the fractions of C4 and C5 against the boilup ratio, the graphs looked similar as figure 3.7 with an intersection where there was good separation of both light and heavy key.

Table 3.6: Different configurations for distillation column 2.

P (bar)	**RR**	**BR**	**C4TOPFR**	**C5BOTFR**	**T** (°C)
1	0.1	0.26	0.95	0.26	61
1	0.5	0.36	0.95	0.26	50
1	0.8	0.41	0.97	0.24	50
5	0.2	0.52	0.95	0.22	96
5	0.5	0.55	0.95	0.22	107
5	1.0	0.56	0.95	0.22	109
5	1.5	0.78	0.97	0.26	25
10	1.0	0.36	0.95	0.16	126
10	1.5	0.48	0.96	0.30	25
15	1.0	0.81	0.99	1.00	36
15	1.5	2.06	1.00	1.00	37
15	2.0	2.31	1.00	0.99	38

However, having a pressure of 15 bar in the distillation column would be very costly. A pressurized column requires thicker walls to withstand the pressure and needs extra equipment such as pumps or compressors. Also, the reboiler duty increases as the boilup ratio is larger for higher pressures. Therefore, it was decided to have an atmospheric distillation column at 1 bar and accept that the components were not separated properly. The naphtha stream would not contain so much of hydrocarbons lighter than C5, but some of the hydrocarbons heavier than C4 would be present in the gaseous product and therefore the naphtha would have a smaller mass flow.

Since 1 bar was chosen as pressure for the second column, the procedure for choosing the different parameters for the column was conducted with that pressure. The graph that describes the relation between reflux ratio and number of stages was generated with a DSTWU column and is shown in figure 3.8. After choosing number of stages, the sensitivity was then conducted with varying the reflux and boilup ratios, with the constraint that 95% of the n-butane needed to be in the distillate. As is seen in table 3.6, the different reflux ratios did not affect the separation very much, and therefore a low reflux ratio of 0.1 was chosen to minimize the boilup ratio and in extension the energy consumption. Figure 3.9 shows how the boilup ratio affects the mole fractions of n-butane in the top product and n-pentane in the bottom product.

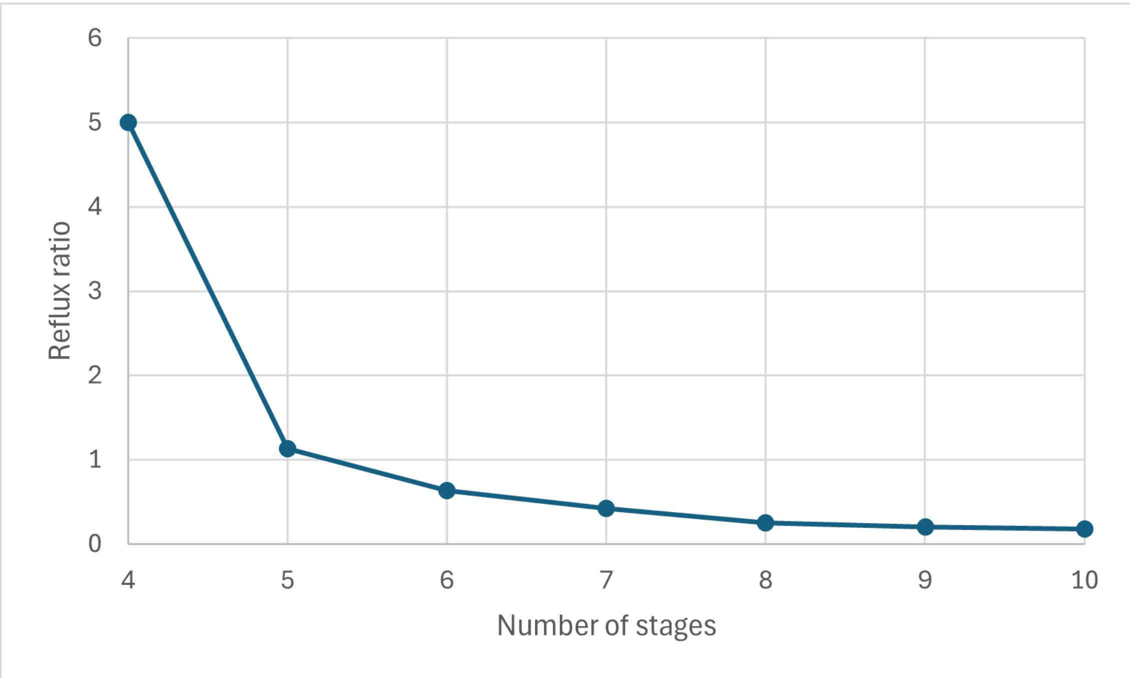

Figure 3.8: Reflux ratio depending on number of stages in distillation column 2.

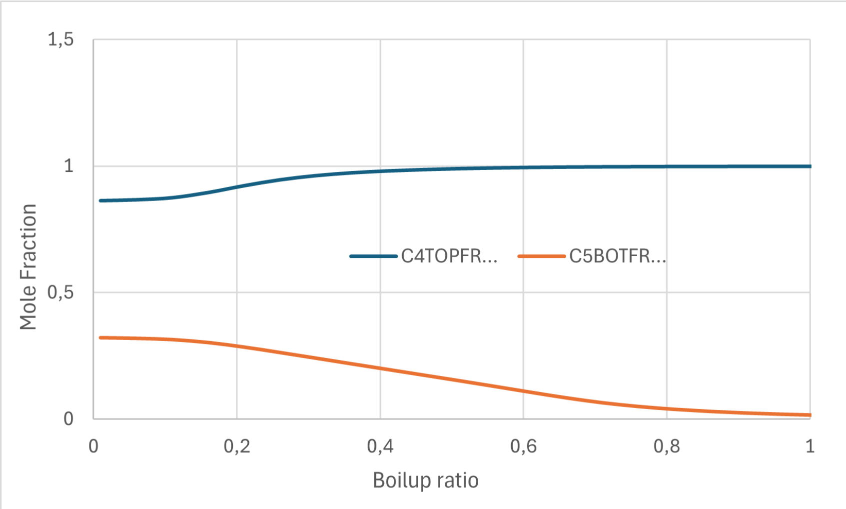

Figure 3.9: Fraction of n-butane (C4) that end up in top product and fraction of n-pentane (C5) that end up in bottom product, when RR=0.1 and BR is varied.

3.4.6 Decanter

Process 3 had a decanter **(14)** after the separation of naphtha, in order to drain the remaining water that was not separated in the first separation step of water.

3.5 Different plastic feedstocks

The processes were designed and optimized for a feedstock of PE. To test how the processes worked with other feedstocks, the feedstock of process 3 was changed to PP and mixed plastcs (DKR-350) respectively.

For the case of a mixed feedstock with DKR-350, the second distillation column did not converge when keeping the process with the same parameters as with a feedstock of PE. To fix the issue, which was that some of the stages dried up, the reflux ratio was simply increased from the original value 0.1 to the slightly higher 0.2. A such slight change to the process was sufficient to make it to run again, indicating that the process was flexible with having some other feedstocks as well.

3.6 Energy analysis

Even if the pyrolysis reactor was outside of the scope of this project, it was interesting to know if the process could be self-sufficient in terms of energy. Especially, if the light gases could provide sufficient energy for heating the plastic waste and the fluidization gas up to 450°C. To first of all know if the separation process was self-sufficient and how much of cold utilities that were needed, a grand composite curve was created with the Aspen Energy Analyzer software. Further an analysis was made with an assumed value of 2.8 MJ/kg for pyrolyzing the plastic waste [31], to see if the light gases could cover the energy demand for heating up the steam and plastic waste. The heat provided from the combusted gas was calculated with equation (3.1), where the values for the gas mass flow and higher heating value were provided from Aspen Plus. The heat required to perform the pyrolysis of the plastic waste was calculated in equation (3.2), while equation (3.3) gave the heat for economizing, evaporating and superheating the steam with the assumption that the feedwater was 25°C. If $Q_{gas} > Q_{plastic} + Q_{steam}$, the light gases provided enough heat to run the process.

$$Q_{gas} = \dot{m}_{gas} HHV_{gas} \tag{3.1}$$

$$Q_{plastic} = \dot{m}_{plastic} * pyrolylsis\ energy\ demand \tag{3.2}$$

$$Q_{steam} = \dot{m}_{steam}(C_{P,water}(100 - 25) + H(1\ bar,\ 450°C) - H_{sat\ liq}) \tag{3.3}$$

3.7 Sizing and economic assessment

3.7.1 Equipment cost

3.7.1.1 Distillation columns

For the sizing of the distillation columns, Aspen Plus automatically calculated the height required for each stage. The number of stages was already chosen, so the height could easily be calculated and one extra meter was added for auxiliary equipment. The diameter was also calculated with Aspen Plus. To know the shell mass, in order to calculate the cost, a proper material needed to be selected. Since the columns as well as the rest of the process were at atmospheric pressure, there was no need for a material that could withstand extreme pressures. Also, the process did not include corrosive fluids. Therefore carbon steel, which is a relatively cheap material, was selected. Carbon steel can withstand temperatures up to 900°F (482°C) which is above the maximum temperature in the process. The wall thickness need to be minimum 1.5 mm for the vessel to carry its own weight, and have a corrosion allowance of 2 mm. To have margin, the wall thickness was set to 5 mm, which is enough for vessels with a diameter of maximum 1 m. With all the dimensions of the vessel defined, the weight could be calculated with the density of carbon steel. Equation (3.4) was used to determine the cost for the vessel based on the shell mass, where the mass was in kg and the cost in USD. Sieved trays were used for the columns, because they were the cheapest type of tray. Equation (3.5) is a cost function for a sieved tray depending on the diameter, where the diameter is in m and the cost is in USD. Both cost functions are for the prices of 2010, so cost index was used later to adjust the cost to today's prices [3]. To obtain the total cost for each distillation column, the cost for the vessel was added to the cost for one tray times the number of trays.

$$Cost_{vessel,cs} = 11600 + 34 * m^{0.85} \tag{3.4}$$

$$Cost_{tray,sieved} = 130 + 440 * d^{1.8} \tag{3.5}$$

3.7.1.2 Flash tanks

The flash tanks needed to be dimensioned with a diameter so that the vapor flow was slow enough to let the liquid droplets settle. Equation (3.6) was used to calculate the settling velocity of the droplets, where ρ_l is the liquid density and ρ_v is the vapor density [3].

$$u_t = 0.07\sqrt{\frac{\rho_l - \rho_v}{\rho_v}} \tag{3.6}$$

To calculate a diameter that was large enough for the vapor flow to slow down below the settling velocity of the droplets, equation (3.7) was used, where V_v is the vapor volumetric flow rate. All flash tanks were assumed to have demister pads, and in that case $u_s = u_t$ (otherwise, $u_s = 0.15u_t$) [3].

$$D_v = \sqrt{\frac{4V_v}{\pi u_s}} \tag{3.7}$$

For the height of the vessel, the liquid depth needed to be known. A holdup time of 10 minutes was assumed, so with the holdup time, the liquid volumetric flow rate and the diameter of the vessel the liquid depth could be calculated. 0.6 m of height was added as a margin between the liquid level and the inlet. Above the inlet, 1.0 m of margin was added between the inlet and the demister pad, and the demister pad was assumed to be 0.4 m high. The wall thickness was also assumed to be 5 mm and the material carbon steel, just as for the distillation columns. With all dimensions and the density of carbon steel, the weight of the vessel could be calculated and equation (3.4) was used to the determine the cost for each flash tank [3].

3.7.1.3 Decanter

A decanter was used to separate the remaining water from the naphtha at the end of process 3. For the dimensioning of the decanter, it was assumed that the vessel was cylindrical and vertical. The naphtha was treated as the continuous phase since that was the largest mass flow of the two phases, while the water was treated as the dispersed phase. The decanter was dimensioned with the condition that the velocity of the continuous phase was less than the settling velocity of the dispersed phase, which is shown in equation (3.8) where u_c is the velocity of the continuous phase, L_c is the continuous phase volumetric flow rate, A_i is the area of interphase between the continuous and dispersed phases and u_d is the settling velocity of the dispersed phase droplets [3].

$$u_c = \frac{L_c}{A_i} < u_d \tag{3.8}$$

The settling velocity of the dispersed phase was calculated with Stokes' law (3.9) where d_d is the droplet diameter of the dispersed phase, g is the gravitational acceleration, ρ_d is the density of the dispersed phase, ρ_c is the density of the continuous phase and μ_c is the viscosity of the continuous phase. The droplet diameter of the dispersed phase was assumed to be 150 μm [3].

$$u_d = \frac{d_d^2 g(\rho_d - \rho_c)}{18\mu_c} \tag{3.9}$$

To get the minimum vessel diameter, it was assumed that $u_c = u_d$ and the minimum area of interface was calculated with equation (3.8), and from that, the minimum vessel diameter. For the height of the vessel, a retention time of 2 minutes was assumed and the settling velocity of the dispersed phase was multiplied with the retention time to obtain the height of the dispersion band. It was assumed that the dispersion band was 10% of the total height of the decanter, so the total height was calculated as 10 times the dispersion band. The wall thickness was assumed to be 5 mm for the decanter as well, and equation (3.4) was used to calculate the vessel cost [3].

3.7.1.4 Heat exchangers

Several heat exchangers were used in each of the processes for the streams to reach their target temperatures before entering distillation columns, flash tanks or decanters. To know the amount of heat exchangers and their size, a pinch analysis and a creation of a heat exchanger network would need to be performed as well as design of each heat exchanger. In this project, the scope was not to perform such an extensive heat exchanger network design and therefore the capital cost for the heat exchangers was simply assumed to be 15% of the capital cost of the major equipment.

3.7.2 Fixed capital costs

Apart from the equipment cost, there were fixed capital costs which actually are the majority of the total capital cost. These costs were most easy estimated by multiplying the major equipment cost with certain factors, since the exact amounts of the fixed capital costs were difficult to estimate. The factors for each item are shown in table 3.7, which are specific for a process with only fluids. The first six factors were for the inside battery limits investment (ISBL), and the sum of the ISBL cost factors included the cost of the major equipment. Apart from those, there were additional costs for offsites, design and engineering and contingency. In total, the total capital cost was 3.9 times the cost of the major equipment.

Table 3.7: Factors for Estimation of Project Fixed Capital Cost [3].

Item	Factor
f_{er} Equipment erection	0.3
f_p Piping	0.8
f_i Instrumentation and control	0.3
f_e Electrical	0.2
f_c Civil	0.3
f_s Structures and buildings	0.2
f_l Lagging and paint	0.1
ISBL cost (including major equipment)	**3.2**
Offsites (OS)	0.3
Design and Engineering (D&E)	0.3
Contingency (X)	0.1
Total capital cost	**3.9**

Additionally, a working capital was needed which made up for raw material inventory, product inventory, cash on hand, spare parts inventory and accounts for receivable products and payable feedstocks. This was estimated as 5% of the total fixed capital cost.

3.7.3 Operational cost

3.7.3.1 Utilities

The operational costs consisted of utilities and fixed operational costs. In this type of process, cooling water was considered as the only utility needed since the process was self-supportive in terms of heat. The heat from the process could also be sold as district heating or process steam depending on the plant location, but since the location of the plant was not known it was assumed that only cooling water was used for cooling. This could therefore be considered as a "worst case scenario" in terms of utilities, where no benefit was drawn from the excess heat. The price of cooling water from Aspen Plus was used, which was 0.76 USD/MWh, and an operational time of the plant was assumed to be 8000 h/year. The price for plastic feedstock can be both positive and negative depending on the demand, so for simplicity the price was assumed to be 0. Since the whole process was at atmospheric pressure, there was no need for pumps to elevate the pressure and the pump and electricity costs were therefore neglected.

3.7.3.2 Fixed operational costs

Apart from utilities, the operating costs also consisted of fixed operating costs that remained the same regardless of the plant's production. Table 3.8 shows the fixed operating costs that are considered in this project, and how they depend on either the capital or the labor cost. For the labor, it was assumed that the plant could be operated by two people since it was a rather small plant, and that they worked in four shifts which gave a total of 8 operators. The salary of each operator was assumed to be 40000 SEK/month and costs for allowances were 45% of the salary.

Table 3.8: Fixed operating costs [3].

Fixed operating costs	Factor
Maintenance	3% of capital cost
Lab cost	22% of labor cost
Supervision	25% of labor cost
Management	40% of labor and supervision costs
Rate on capital	10% of capital cost
Insurance and taxes	1% of capital cost

3.7.4 Economic evaluation

For the economic evaluation, it was assumed that 40% of the capital cost is payed in 2025, 50% in 2026 and 10% in 2027. The whole working capital is payed in 2027, which is also the year when the plant is starts to operate. The operating cost is increasing for each year because of the time value of money, where the interest rate r was assumed to be 5%.

To annualize the capital cost, an annuity factor was calculated with equation (3.10). n is the lifetime of the plant, which was assumed to be 20 years. The capital cost was then divided with the annuity factor to obtain the annual capital cost. The total annual cost was then calculated by adding the annual capital cost with the operational cost.

$$Annuity\ Factor = \frac{1-(1+r)^{-n}}{r} \tag{3.10}$$

To calculate the price for separating the products, it was assumed that diesel and naphtha were the two valuable products obtained from the process. As stated before, the light gases were combusted to provide the pyrolysis reactor with heat so they were not considered as a product that could be sold. The waxes were not used for anything, because their value was considered to be much lower than naphtha and diesel so they were neglected in these calculations. The prices for naphtha and diesel are very volatile and change depending on the market. Therefore, for simplicity it was assumed that they had the same price when calculating the separation cost. The total annual cost was divided between the production of naphtha and diesel, and in this way a cost for the separation process was obtained with the unit SEK/ton.

4
Results and discussion

4.1 Separation steps

Table 4.1 shows a summary for all the separation steps that involved flash tanks. In the same way, table 4.2 show the results for the distillation columns. The results are for a PE feedstock, which was used to evaluate the three processes and compare them against each other.

Table 4.1: Results from the separations steps with flash tanks.

Number in flowsheet	**T (°C)**	**Fraction of target components separated**	**Purity of liquid product**
2	160	91%	77%
4	50	97%	100%
6	25	92%	91%
8	110	92%	49%
10	25	77%	91%

Table 4.2: Results from the separation steps with distillation columns.

Number in flowsheet	11	13
Number of stages	17	7
Reflux ratio	0.2	0.1
Boilup ratio	8.7	0.26
Fraction of target components separated	89%	91%
Purity of bottom product	78%	95%

4.1.1 Separation of waxes

For the separation of waxes **(2)**, it was decided from figure 3.4 to have a temperature of 160°C in the flash tank. With that temperature, 91% of the waxes are separated. However, the wax stream contains of 77% waxes while the rest are mostly diesel components that are condensed along with the waxes, which can be seen in figure B.1.

4.1.2 Separation of water

The temperature for the flash tank that separates the water **(4)** was chosen to be 50°C. As seen in table 4.1, the purity of the water was 100% (with only small traces of hydrocarbons <0.01%). The purity of the separated water was actually independent of the temperature, so there was no drawback in going down in temperature. With the selected temperature, 97% of the water was separated.

4.1.3 Separation of oil

The separation between pyrolysis oil and light gases in process 1 **(6)** was performed at ambient temperature (25°C), since the purpose of that separation was just to condense all the condensable products. Of the target components in the feed to the flash tank (naphtha and diesel components), 92% were condensed to the liquid phase and the obtained pyrolysis oil had a purity of 91%. A detailed composition of the oil and gas streams can be seen in figures B.2 and B.3.

4.1.4 Separation of diesel

For the separation of diesel, process 2 used a condenser with flash tank **(8)** and process 3 used a distillation column **(11)**.

4.1.4.1 Flash tank

The temperature of the flash tank for the separation of diesel was set to 110°C. This is an increase of 60°C from the previous separation step (separation of water), which was at 50°C. At this tempeature, 92% of the diesel was separated. However, the purity of the diesel was only 49%, with many of the naphtha components being condensed together with the diesel. If the temperature would be higher, the separated diesel would have higher purity but that would mean that the naphtha would contain more of the diesel components. Since the main product in this separation process is naphtha, a high temperature was chosen to obtain a high purity of naphtha even if the diesel product then has lower purity.

4.1.4.2 Distillation column

The number of stages was set to 17 stages, where the reflux ratio does not get much lower according to figure 3.6. After testing different reflux and boilup ratios, a boilup ratio of 8.7 was chosen according to figure 3.7 where the curves cross each other. The figure was created with a reflux ratio of 0.2, which was the lowest reflux ratio possible and still have over 95% recovery of the light and heavy keys. The lowest reflux ratio also gave the lowest boilup ratio, and thus the lowest energy consumption. With this configuration of the distillation column, 89% of the diesel was separated with a purity of 78%. The composition of the diesel product stream is shown in figure B.4. Apart from the waxes, other impurities that the stream contains are some amounts of C12 components.

4.1.5 Separation of naphtha

The separation of naphtha was performed with either a cooler and flash tank **(10)** in process 2, or with a distillation column **(13)** in process 3.

4.1.5.1 Flash tank

With a flash tank, the temperature was lowered to ambient temperature (25°C) to condense the naphtha and leave the rest of the components in vapor phase. 77% of the naphtha was condensed, with a purity of 91%.

4.1.5.2 Distillation column

In a similar way as the first distillation column, the number of stages was determined to 7 stages where "the curve gets flat" in figure 3.8. A low reflux ratio of 0.1 was chosen to minimize the boilup ratio and in extension the energy consumption. In figure 3.9, it is seen that there is no intersection between the curves as it was for the first column. Since a 95% of n-butane in the distillate was set as a constraint, the boilup ratio was decided to be 0.26. With this configurations, the distillation column could separate 91% of the naphtha with a purity of 95%. The component distribution of the naphtha is shown in figure B.5. The target components, C5-C12, are mostly the main components of the stream, but also some of C13. As shown in the graph, most part of the compounds are n-paraffins and α-olefins, and some iso-olefins too.

4.1.6 Decanter

The decanter separates away the remaining water from the naphtha product. Before the decanter, the stream consisted of 4.5 wt% water. After the separation, the naphtha stream had only 0.9 wt% water.

4.2 Energy analysis

Figure 4.1 shows the grand composite curve of process 3 (blue graph) and the utilities (red graph) that the process can generate or are needed. From the graph it is seen that the separation process is self-supportive in terms of heat, but what needs to be taken into consideration is that the pyrolysis reactor is not included in the system, so the inlet stream to the process is already 450°C. What can also be seen is that the process can generate some amounts of HP, MP and LP steam, which can be generated and sold to other plants nearby if there is any demand for that. The process could also generate district heating, if the plant is located in an area that has such demand. Since the plant location is not known though, it is assumed that only cooling water is used to cool down the process.

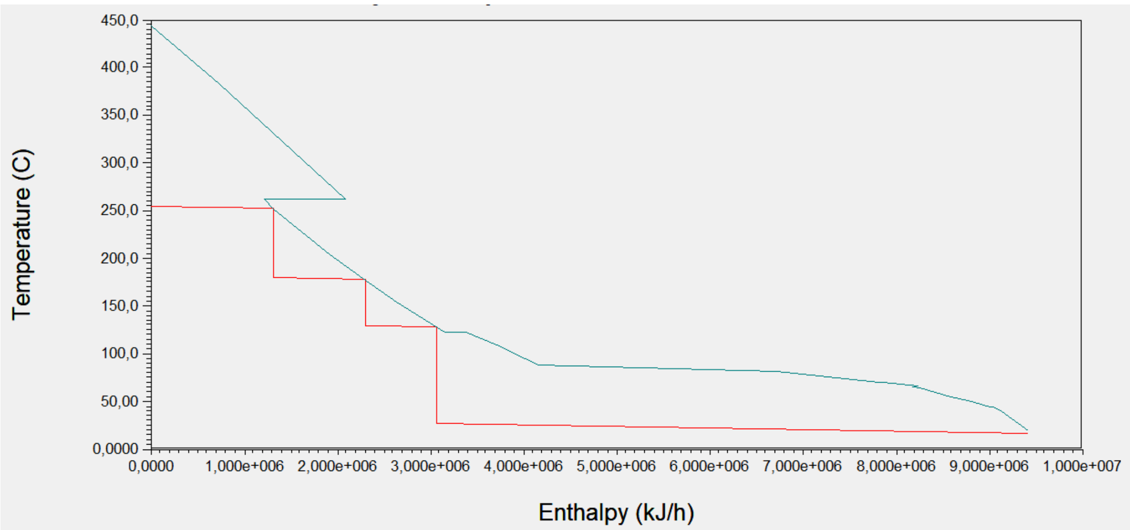

Figure 4.1: Grand composite curve with utilities.

Table 4.3 shows the amount of heat provided by combusting the light gases from process 3, and the heat required to pyrolyze the plastics and superheat the fluidization steam. What can be seen is that the amount of heat from the gases is more than enough to heat up the plastics and steam, so the process can be completely self-sufficient in terms of heat if the light gases are combusted.

Table 4.3: Heat provided from combusting gases and required to pyrolyze plastic and superheat steam.

Stream	Energy (MW)
Q_{gas}	5.8
$Q_{plastic}$	1.9
Q_{steam}	1.8

4.3 Different plastic feedstocks

The results for each process have so far been evaluated with a PE feedstock. This section evaluates how a change of feedstock affects the product streams. For this evaluation, process 3 was used.

4.3.1 Polypropylene

PP contains more of heavy waxes than PE, so the wax stream when PP is used as feedstock in the process has considerably more of C30 and heavier components than with PE. The reason for the high amount of waxes could be that since PP has a methyl group attached to every second carbon atom, there molecules are much heavier than for an equally long PE polymer chain [4]. The separation works rather well with the same temperature in the flash tank as for PE, with small amounts of lighter components down to C15 that follows with the wax, which is seen in figure B.7. The first distillation column has diesel as bottom product, and for PP as feedstock the distribution of components in the diesel product stream is as in figure B.8. Apart from the target components C13-C19, the stream contains some waxes of C20 and heavier, and a large amount of C12 which in the case of PP seems to end up in the diesel product stream instead of in the naphtha. Figure B.9 shows the distribution between the components of naphtha, and it can be seen that almost the whole stream consist of iso-olefins, and the largest component is C9. Other components that there is much of and should be in the naphtha stream are C6 and C12, but those are instead found in the gas and diesel streams respectively. Even if there is a big loss of naphtha in the form of C6 and C12, the naphtha stream has a high purity with practically no no components outside the naphtha range. Finally the rest of the components after the naphtha has been separated are shown in figure B.10, and what can be seen here is that C3 and C6 dominate. In the case of C3 it consist completely of propylene and for C6 it is a mixture of different compounds, but mostly of iso-olefins which in this case was modeled as 2-methyl-1-pentene.

4.3.2 Mixed plastics

The simulation of mixed plastics was made by using the composition of DKR-350, which is described in the method chapter. What can be seen in the figures for the product streams is that the oxygenates from PET are present in all streams. In the wax stream in figure B.11 there is is a mass flow of terephthalic acid that is almost as large as the mass flow of C30-C39 waxes, with minor amounts of other acids as well. The diesel stream in figure B.12 contains even more acids, with benzoic and toluic acids being the two largest components after C15-C16 hydrocarbons. It also contains polyaromatics, such as diphenyl and terphenyl. The naphtha product stream in figure B.13 show that also this stream is contaminated with benzoic acid, and also have more aromatics than PE. The large amount of aromatics consist of a large share of styrene, which comes from the fraction of PS in the mixed plastics. For the aliphatic components, the separation is still almost equally good as for PE with the exception that there are more C13-C14 components. The light gases in figure B.14 have a large variety of components, including acetaldehyde, carbon dioxide, carbon monoxide and water. Since the gases are going to be burnt anyway to provide heat for the pyrolysis process, the fact that it is a mixture of many different components does not matter that much as for the impurities of the other streams.

4.3.3 Comparison between different plastic feedstocks

As discussed previously for each plastic feedstock, the separation process which was originally designed for PE works to different extents with other feedstocks. Figure 4.2 has the mass flows of naphtha and diesel for the different feedstocks, which are the main product and the most valuable by-product respectively. The target components are the hydrocarbons that are supposed to be present in each product (C5-C12 for naphtha and C13-C19 for diesel), while the untarget components are the rest of the hydrocarbons present and the impurities are oxygenates and water. What is interesting to see is that the process actually gives a both higher and cleaner yield of naphtha for PP than for PE, even if the process originally was designed for PE.

This probably depends on that the pyrolysis products of PP consist of iso-olefins to a large extent, with very small amounts of impurities. Therefore, it should not be a problem to switch between PE and PP feedstocks. Also, assuming that the pyrolysis products of mixed PE and PP have a linear relationship to the pyrolysis products of pure PE and PP respectively, the process would be able to handle a mixture of PE and PP without any major impacts on the product quality.

When comparing the streams from the DKR-350 feedstock with the streams from PE and PP though, it is clear that the products will contain more impurities when having a mixture with different plastics. The impurities are of mostly oxygenates such as benzoic acid. A product with lower purity will of course have to be sold at a lower price than a product with higher purity, so the alternatives are either accepting the low purity sell the product at a lower price, having to pre-sort the plastic waste to have a stream that does not contain PET, or modify the separation process to be able to separate oxygenates from the rest of the mixture.

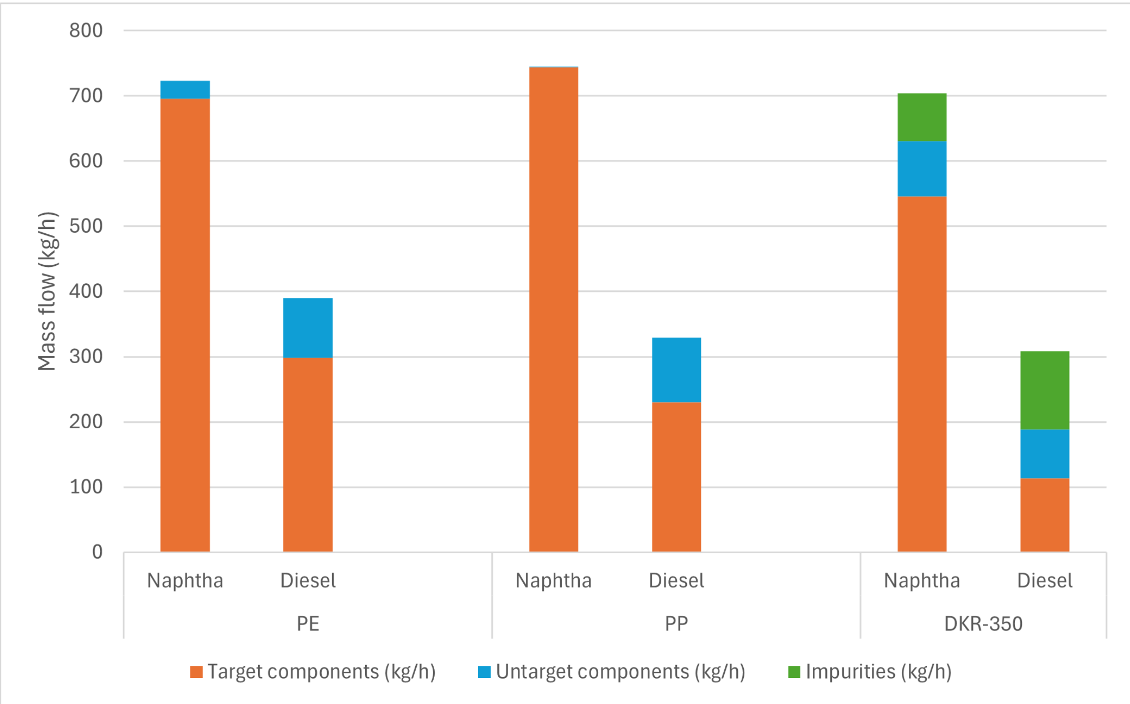

Figure 4.2: Naphtha and diesel product streams from different feedstocks.

4.3.4 Alternative separation methods

Separation by boiling point does not seem to work for separating carboxylic acids and other oxygenates from pyrolysis oil, so if the process were to be modified or extended with additional separation steps, other separation methods would need to be considered. One method is solvent extraction, where the the mixture that contains the carboxylic acids is mixed with a solvent that is soluble with the carboxylic acids, but not with the rest of the hydrocarbons. Hizaddin et al. investigated the possibility of using deep eutectic solvents to separate phenols from non-polar aliphatic and aromatic components. Their results showed that it was possible to extract a large amount of phenol in one single extraction stage, using the deep eutectic solvents [32]. Phenols are different than carboxylic acids, but they are both polar so there can be some similarities in separating out phenols or carboxylic acids.

4.4 Process comparison

In this section, the three different processes are compared in terms of the yield and purity of the products, as well as for the economics.

4.4.1 Product stream compositions

The product streams from the different processes that were simulated with a PE feedstock are summarized in figure 4.3. The wax stream is the same for all three processes of course, since all processes have the same temperature in the first flash tank where the wax is separated. After that the products are different though, with process 3 having a smaller but cleaner diesel product than process 2. This is of course because process 3 is using a distillation column to get as high purity as possible for both naphtha and diesel, while the other process uses a heat exchanger with flash tank instead. Process 1 does not separate diesel and naphtha, so instead there is an "oil" product stream which has an equivalent mass flow as the naphtha and diesel streams added for the other processes. When comparing the naphtha streams for process 2 and 3, it is clear that process 3 gives a significant higher amount of naphtha which also has higher purity. The gas streams are rather similar, with process 3 having slightly higher purity. The purity of the gas product is not as important though, since it is combusted to provide the pyrolysis reactor with heat.

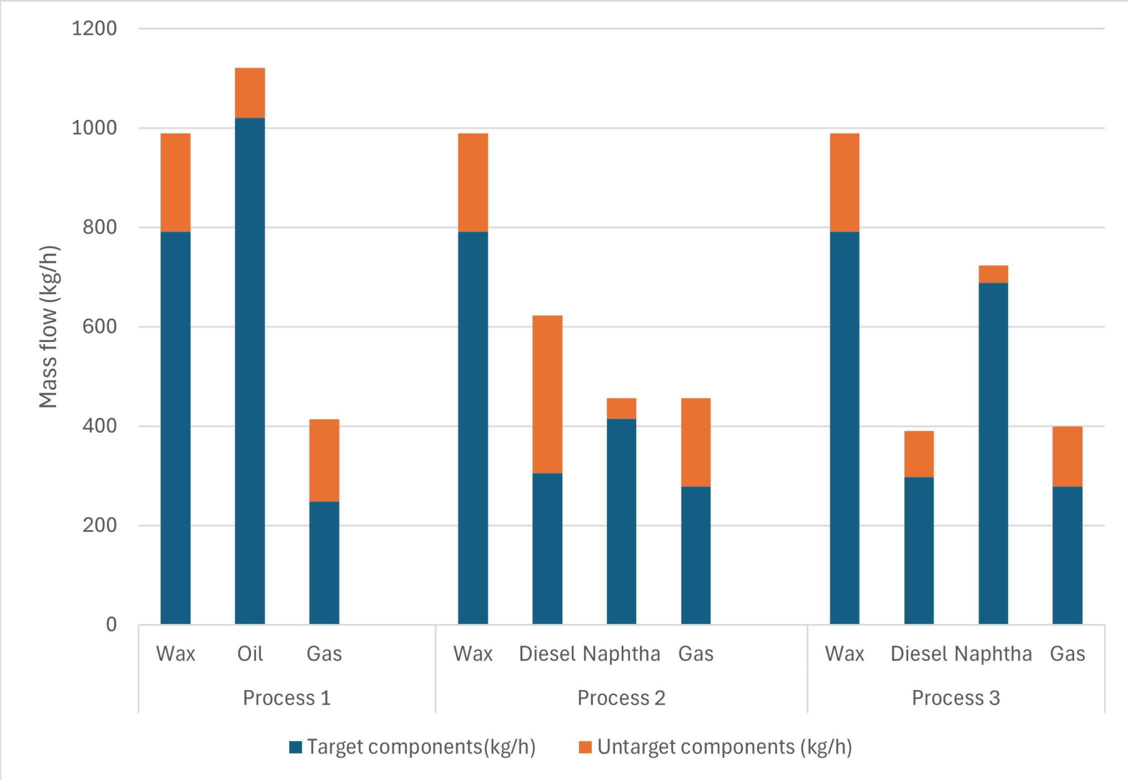

Figure 4.3: Yield of different products from different processes, with PE feedstock.

4.4.2 Sizing and economic assessment

The economic assessment was performed for all three processes, in order to compare the capital and operational costs between them. Tables C.1, C.4 and C.7 show the equipment cost for each unit, in USD and SEK based on cost functions from 2010 so the prices are based on the market of 2010. What is interesting to see is that the prices for each unit is approximately the same for each process (except distillation column 1 process 3) indicating that it is the number of major equipment units that affect the capital cost the more rather than which type of units it is. Process 1 and 2 have less units than process 3 so of course they will be cheaper, but a process is not necessarily cheaper if the distillation columns are replaced by flash tanks. Tables C.2, C.5 and C.8 show the total capital cost and working capital, which change proportionally to the equipment cost for each process. Finally there are operating costs in tables C.3, C.6 and C.9 where the cost of labor and the costs that are based on labor (lab cost, supervision and management) are the same for each process. Since the labor costs are the majority of the operating costs, the total operating costs are very similar for all three processes. The difference depend on the operating costs that depend on the capital cost (maintenance, rate on capital and insurance and taxes) and the variable operating cost which is the cooling water. Actually, process 1 and 2 uses slightly more cooling water than process 3.

To get an overview of the economics for the different processes compared to each other, figure 4.4 shows the capital and operational costs of the processes. As stated before, the capital cost increases with the complexity of the process and the operational cost is almost the same. What is interesting though is that the operational cost is much higher than the capital cost. Considering a plant lifetime of 20 years, the capital cost will in the long run be insignificant in comparison to the operational cost.

When looking at the separation cost for the different products in figure 4.5, it is even more clear that the total cost for the process is almost the same when the capital cost is annualized over 20 years. Comparing process 1 with process 2, the separation cost for oil compared to naphtha and diesel is only 5% lower. When comparing process 2 and 3, the separation cost is only 0.4% lower for having flash tanks instead of distillation columns. Process 3 gives a higher and purer production of naphtha and therefore the small saving that is made from doing a simpler process would not be beneficial. For process 1, the price for the oil is in the same range as the naphtha and diesel prices for the other processes. Considering that the unseparated oil would need to be sold at a lower price than the naphtha and diesel, it can be questioned if it would be beneficial to have a process that does not separate out different fractions from the oil.

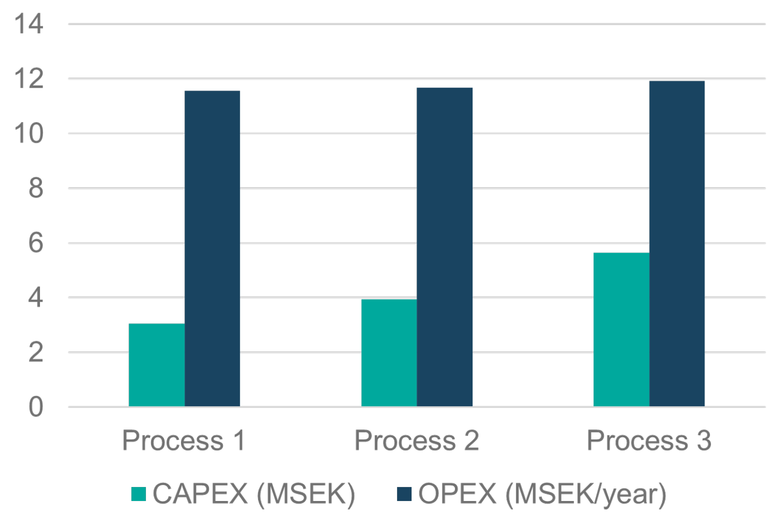

Figure 4.4: CAPEX and OPEX for the processes.

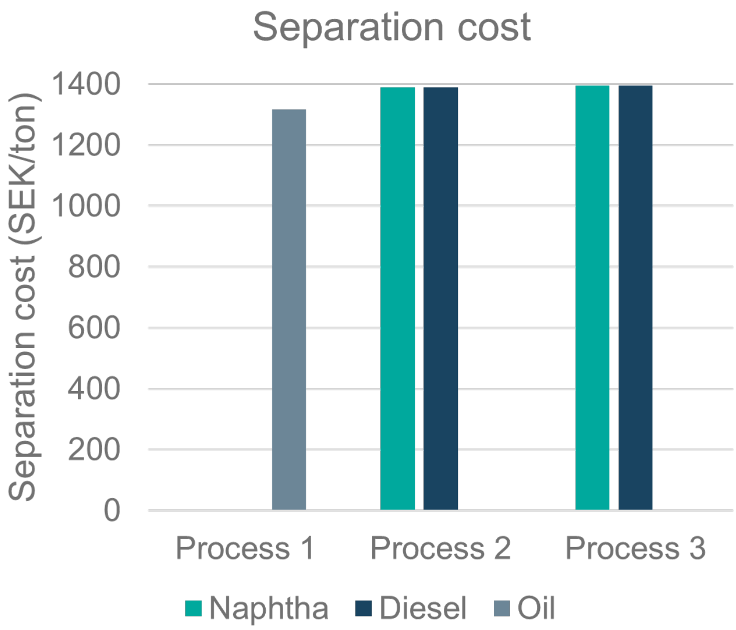

Figure 4.5: Separation cost for the processes.

5
Conclusion

In conclusion, three separation processes for separating condensable products from plastic pyrolysis were created, with special focus on separating the naphtha fraction. Separation of diesel and naphtha fractions was performed using two different ways, flash tanks and distillation columns. Additionally, one process was designed with only separation of pyrolysis oil without separating it into naphtha and diesel. All processes were at atmospheric pressure, since no significant difference was found when the pressure was slightly increased. One would need to increase the pressure above 15 bar to see a significant improvement in the process design.

The results showed that it gave a significantly higher yield of naphtha using distillation columns, with higher fraction of target components. Further it was noticed that all processes had a high yield of wax. When comparing the economics, it was seen that the capital cost increased with an increased amount of equipment, but it was low compared to the operational costs. Since the operational cost mainly depended on the fixed OPEX, it was almost the same for all processes. With these results, it can be concluded that it is more cost-beneficial to build a process with distillation columns that has a proper separation of naphtha and diesel rather than a cheaper process that only uses flash tanks. It can also be concluded that it is more cost-beneficial to separate the naphtha and diesel than having a product of pyrolysis oil, with the assumption that separated naphtha and diesel can be sold at a higher price.

The energy analysis performed for the process with distillation columns showed that combustion of the non-condensable gases can support the pyrolysis reactor with heat. In that sense, the whole process is self-supportive in terms of energy. The feedstock was changed to other plastic waste streams than PE for the process using distillation columns. For a feedstock of PP, the process worked and gave a higher yield of naphtha with higher fraction of target components than for PE. However, it has to be kept in mind that PP yields a high amount of olefins, and it has to be investigated how that affects the further downstream treatment before entering a steam cracker. It was also tested how a change to mixed plastic waste feedstock impacted the process, more specifically DKR-350. The process worked with a slight change by increasing the boilup ratio in the second distillation column. However, PET is a major issue since it yields large amount of oxygenates such as benzoic acid that distributes itself in various of the product streams. Because of this, PET would either need to be pre-sorted before the other mixed plastics enter the pyrolysis reactor, or there would need to be an additional separation step that can remove the oxygenates that have their origin in PET.

5.1 Future work

When doing further work on this topic, several objectives could be explored:

- Alternative separation methods for the separation of oxygenates such as carboxylic acids could be investigated. One such method could be solvent extraction, which could be an additional step after the distillation. PET will always be a component in mixed plastic waste, so not having to pre-sort it before sending the waste to a pyrolysis reactor would facilitate the management of waste plastics.
- The system boundaries could be extended, to include the pyrolysis reactor also. If this is simulated together with the combustion of the light gases, it can be verified if the heat from the combusted gases covers the heat demand for the pyrolysis and fluidization steam production.
- The system boundaries could be extended downstream as well, to include the steam cracker and eventual pre-treatment steps. In this way, a complete techno-economic analysis of the olefin production could be performed to have a better understanding of how pyrolysis of plastic waste could compete with other olefin production pathways.
- To have more reliable results regarding the simulation of mixed plastic waste, experiments could be performed in a pyrolysis reactor with such mixed waste to not rely on data from individual plastics.

Bibliography

[1] H. Jung and Y. Ahn, "Process design for plastic waste pyrolysis: Yield analysis and economic assessment," *Computers and chemical engineering*, 2025.

[2] S. Papari and K. Hawboldt, "A review on condensing system for biomass pyrolysis process," *Fuel processing technology*, 2018.

[3] G. Towler and R. Sinnott, *Principles, Practice and Economics of Plant and Process Design*. Elsevier, 2013.

[4] M. Kusenberg, A. Zayoud, M. Roosen, T. Dao Hang, M. Seifali Abbas-Abadi, A. Eschenbacher, U. Kresovic, S. De Meester, and K. M. Van Geem, "A comprehensive experimental investigation of plastic waste pyrolysis oil quality and its dependence on the plastic waste composition," *Fuel Processing Technology*, 2021.

[5] J. Eun Lee, D. Lee, J. Lee, and Y.-K. Park, "Current methods for plastic waste recycling: Challenges and opportunities," *Chemosphere*, 2024.

[6] K. Ragaert, L. Delva, and K. Van Geem, "Mechanical and chemical recycling of solid plastic waste," *Waste Management*, 2017.

[7] G. J. Antos and A. M. Aitani, *Catalytic Naphtha Reforming*. Marcel Dekker, 2004.

[8] "Diesel and gasoline." `https://www.iea-amf.org/content/fuel_information/diesel_gasoline/`. Accessed: 2025-05-20.

[9] T. Ren, M. Patel, and K. Blok, "Olefins from conventional and heavy feedstocks: Energy use in steam cracking and alternative processes," *Energy*, 2006.

[10] M. Driffield, "New eu regulation targets recycled plastics in fcms." `https://www.exponent.com/article/new-eu-regulation-targets-recycled-plastics-fcms`, 2022. Accessed: 2025-05-13.

[11] "Polyethylene terephthalate (pet) – applications and recycling." `https://polymer-search.com/polyethylene-terephthalate-pet-applications-and-recycling/`. Accessed: 2025-05-13.

[12] "Polystyrene: From production to end-use applications." `https://petropanic.com/en/polystyrene-from-production-to-end-use-applications/`. Accessed: 2025-05-13.

[13] H. C. Genuino, M. Pilar Ruiz, H. J. Heeres, and S. R. Kersten, "Pyrolysis of mixed plastic waste (dkr-350): Effect of washing pre-treatment and fate of chlorine," *Fuel Processing Technology*, 2022.

[14] L. Yang, X. Chen, C. Huang, S. Liu, B. Ning, and K. Wang, "A review of gas-liquid separation technologies: Separation mechanism, application scope,

research status, and development prospects," *Chemical Engineering Research and Design*, 2024.

[15] Y. H. Chan, S. K. Loh, B. L. F. Chin, C. L. Yiin, B. S. How, K. W. Cheah, M. K. Wong, A. C. M. Loy, Y. L. Gwee, S. L. Y. Lo, S. Yusup, and S. S. Lam, "Fractionation and extraction of bio-oil for production of greener fuel and value-added chemicals: Recent advances and future prospects," *Chemical Engineering Journal*, 2020.

[16] N. Abdullah, N. Putra, I. I. Hakim, and R. A. Koestoer, "A review of improvements to the liquid collection system used in the pyrolysis process for producing liquid smoke," *International Journal of Technology*, 2017.

[17] W. Kaminsky, "Chemical recycling of plastics by fluidized bed pyrolysis," *Fuel Communications*, 2021.

[18] M. Lee, H. Ko, and S. Oh, "Pyrolysis of solid recovered fuel using fixed and fluidized bed reactors," *Molecules*, 2023.

[19] "Aspen plus." `https://www.aspentech.com/en/products/engineering/aspen-plus`.

[20] "Aspen energy analyzer." `https://www.aspentech.com/en/products/engineering/aspen-energy-analyzer`. Accessed: 2025-06-04.

[21] W. Zeb, T. De Somer, M. Roosen, P. Knockaert, M. Seifali Abbas-Abadi, U. Kresovic, J. Hogie, K. M. Van Geem, and S. De Mester, "Fractional distillation of waste plastic pyrolysis oil for isolating narrow hydrocarbon cuts," *Fuel*, 2025.

[22] P. T. Williams and E. A. Williams, "Fluidized bed pyrolysis of low density polyethylene to produce petrochemical feedstock," *Journal of Analytical and Applied Pyrolysis*, 1999.

[23] G. K. Parku, F.-X. Collard, and J. F. Görgens, "Pyrolysis of waste polypropylene plastics for energy recovery: Influence of heating rate and vacuum conditions on compositions of fuel product," *Fuel Processing Technology*, 2020.

[24] X. Lian, S. Wang, R. Shan, J. Gu, C. Zhao, W. Zhao, H. Yuan, and C. Yong, "Pyrolysis characterization and mechanism studies of different structural plastics: A comperative study at optimal temperatures," *Energy*, 2024.

[25] A. Zayoud, H. D. Thi, M. Kusenberg, A. Eschenbacher, U. Kresovic, N. Alderweireldt, M. Djokic, and K. M. Van Geem, "Pyrolysis of end-of-life polystyrene in a pilot-scale reactor: Maximizing styrene production," *Waste Management*, 2022.

[26] D. Royuela, A. Veses, J. D. Martínez, M. S. Callén, J. M. López, T. García, and R. Murillo, "Thermochemical recycling of polystyrene waste by pyrolysis using a pilot-scale auger reactor: Process demonstration in a relevant environment," *Resources, Conservation and Recycling*, 2024.

[27] K.-B. Park, Y.-S. Jeong, B. Guzelciftci, and J.-S. Kim, "Two-stage pyrolysis of polystyrene: Pyrolysis oil as a source of fuels or benzene, toluene, ethylbenzene and xylenes," *Applied Energy*, 2020.

[28] A. Dhahak, G. Hild, M. Rouaud, G. Mauviel, and V. Burkle-Vitzthum, "Slow pyrolysis of polyethylene therephthalate: Online monitoring of gas production and quantitative analysis of waxy products," *Journal of Analytical and Applied Pyrolysis*, 2019.

[29] H. C. Genuino, M. Pilar Ruiz, H. J. Heeres, and S. R. Kersten, "Pyrolysis of mixed plastic waste: Predicting the product yields," *Waste management*, 2023.
[30] H. K. V. Gurram, S. H. Pamu, and S. A. Singh, "Parametric studies on fractionation column design for the separation of plastic waste pyrolysis oil into valuable fuels," *Journal of Environmental Chemical Engineering*, 2024.
[31] J. Wu, H. Radhakrishnan, C. H. Oi, O. Olafasakin, J. Brown, K. Nelson, R. Brown, X. Bai, I. Hermans, M. M. Writght, H. A. Aguirre-Villegas, and G. W. Huber, "Pyrolysis of plastic waste: Recycling hard-to-recycle plastics," *CUWP*, 2023.
[32] H. F. Hizaddin, I. Wazeer, N. A. M. Huzaimi, L. El Blidi, M. A. Hashim, J.-M. Lévêque, and M. K. Hadj-Kali, "Extraction of phenolic compound from model pyrolysis oil using deep eutectic solvents: Computational screening and experimental validation," *Separations*, 2022.

A

Aspen Plus flowsheets

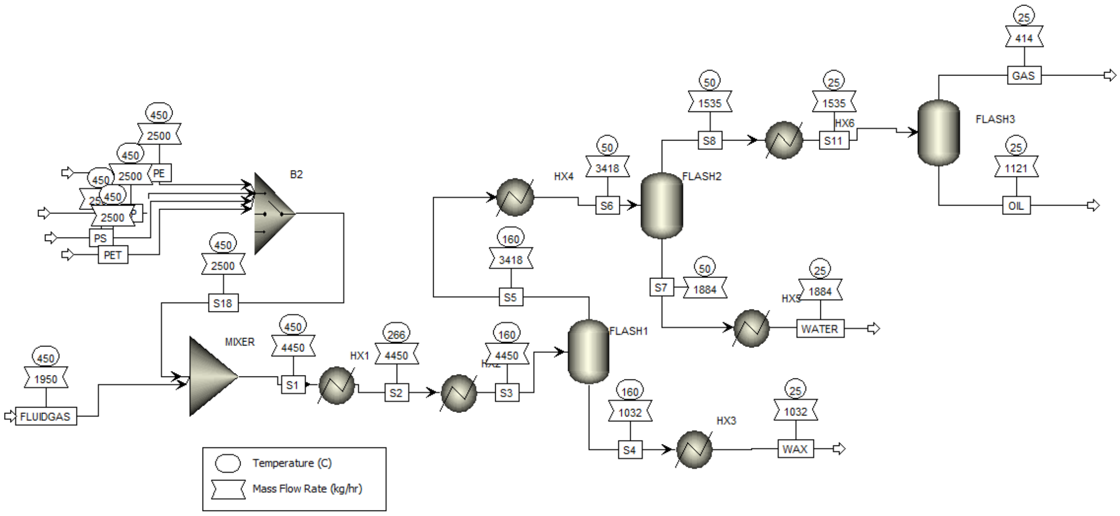

Figure A.1: Flowsheet for process 1 with PE feedstock, with mass flows and temperatures.

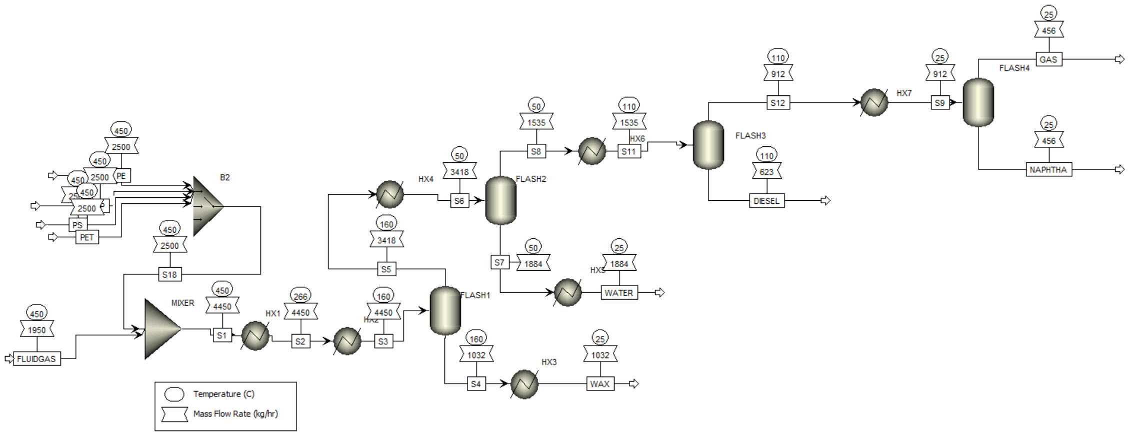

Figure A.2: Flowsheet for process 2 with PE feedstock, with mass flows and temperatures.

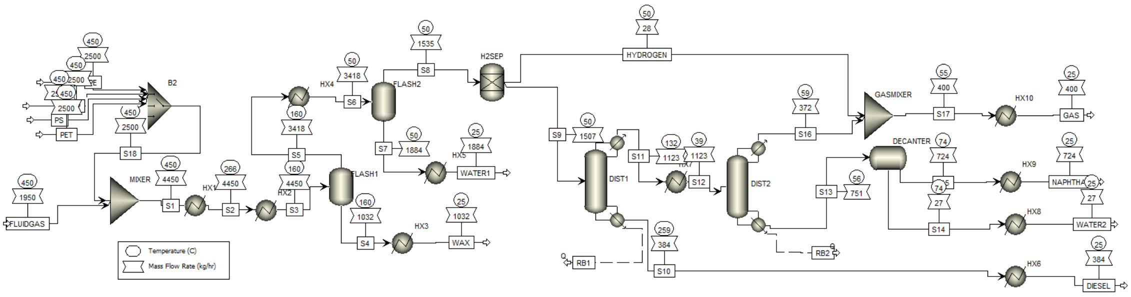

Figure A.3: Flowsheet for process 3 with PE feedstock, with mass flows and temperatures.

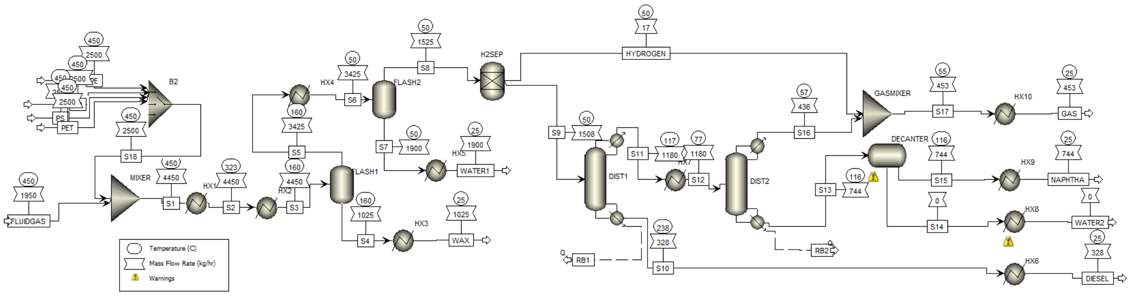

Figure A.4: Flowsheet for process 3 with PP feedstock, with mass flows and temperatures.

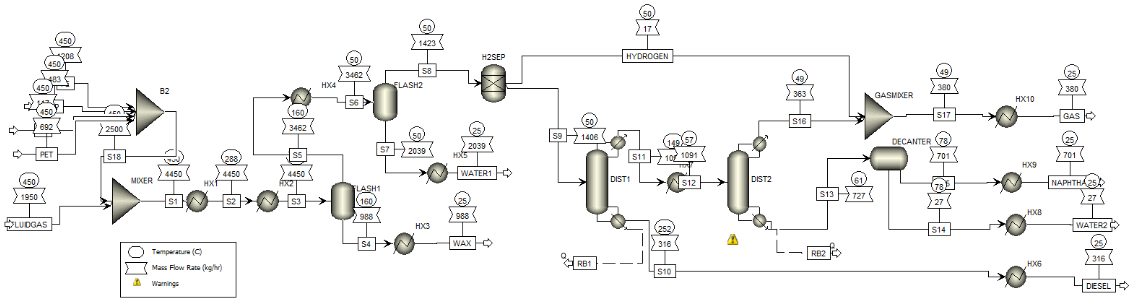

Figure A.5: Flowsheet for process 3 with DKR-350 feedstock, with mass flows and temperatures.

B

Product streams

B.1 PE feedstock

B.1.1 Wax

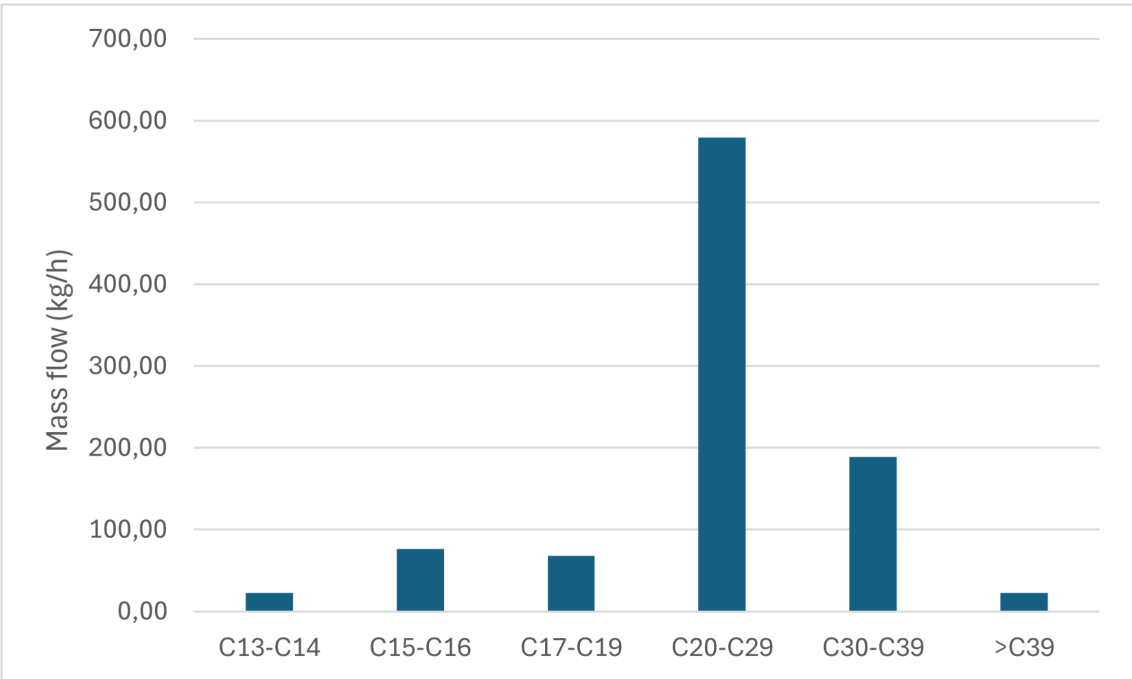

Figure B.1: Distribution of components from wax product stream.

B.1.2 Process 1

B.1.2.1 Oil

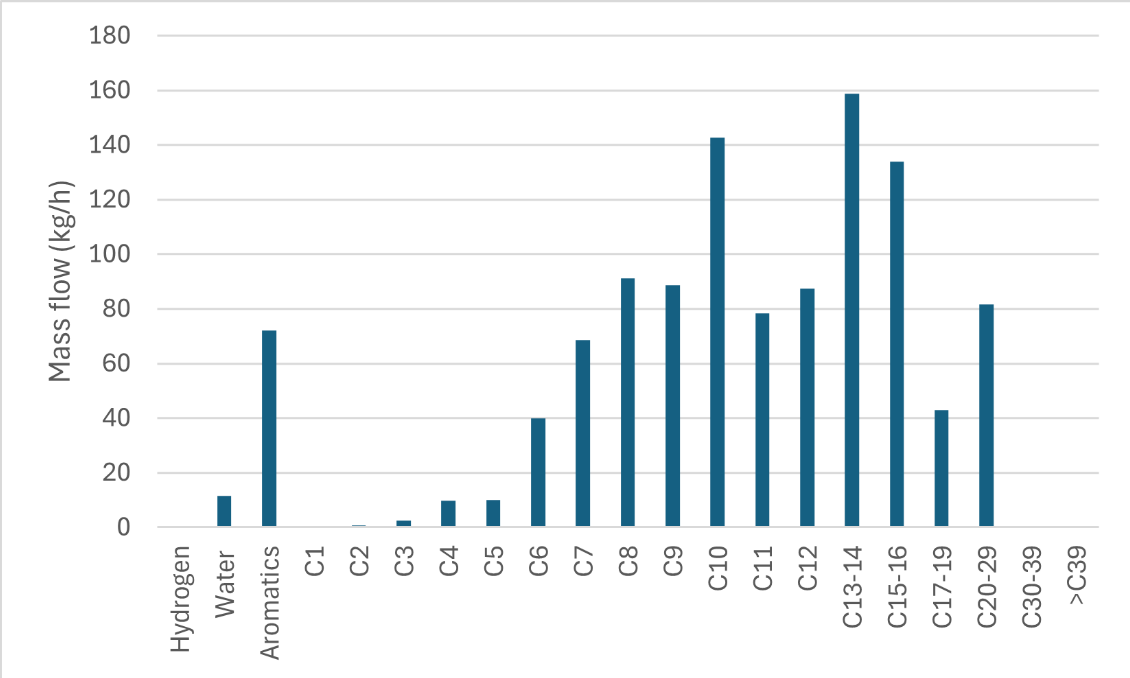

Figure B.2: Distribution of components from oil product stream, process 1, PE feedstock.

B.1.2.2 Light gases

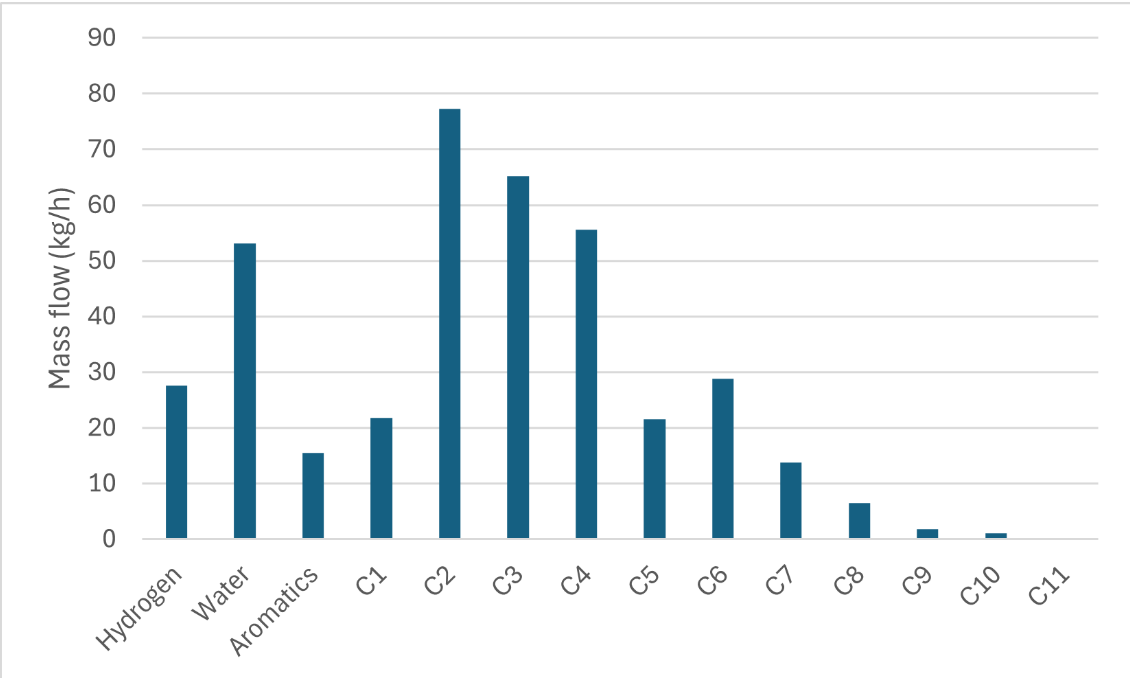

Figure B.3: Distribution of components from gas product stream, process 1, PE feedstock.

B.1.3 Process 3

B.1.3.1 Diesel

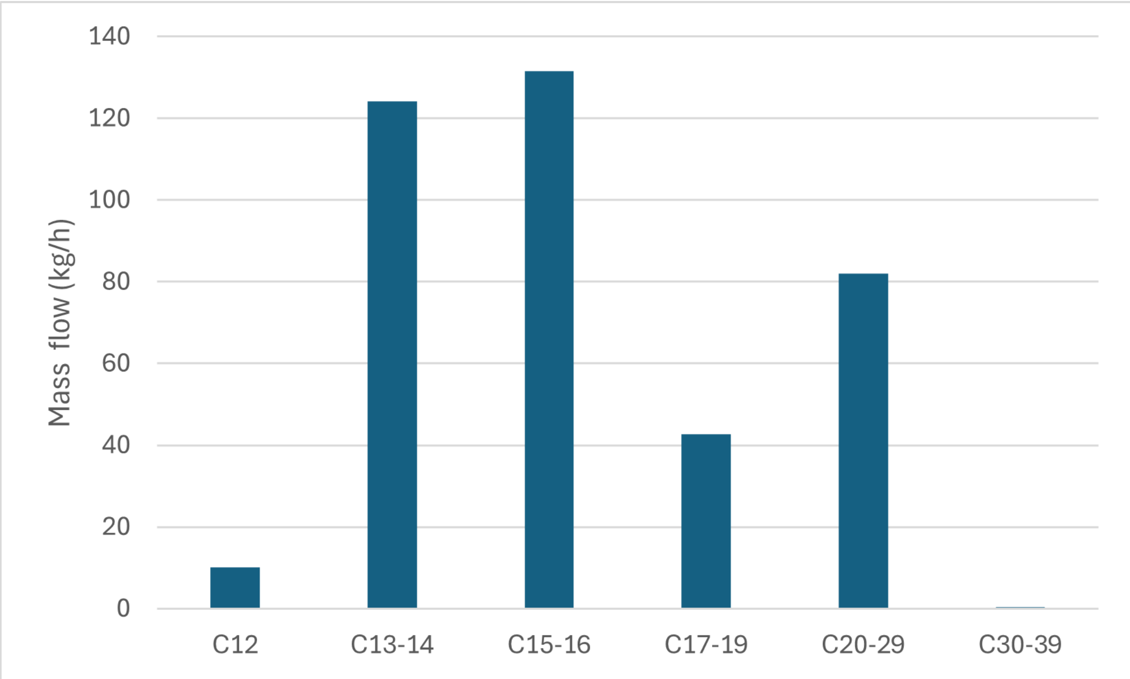

Figure B.4: Distribution of components from diesel product stream, process 3, PE feedstock.

B.1.3.2 Naphtha

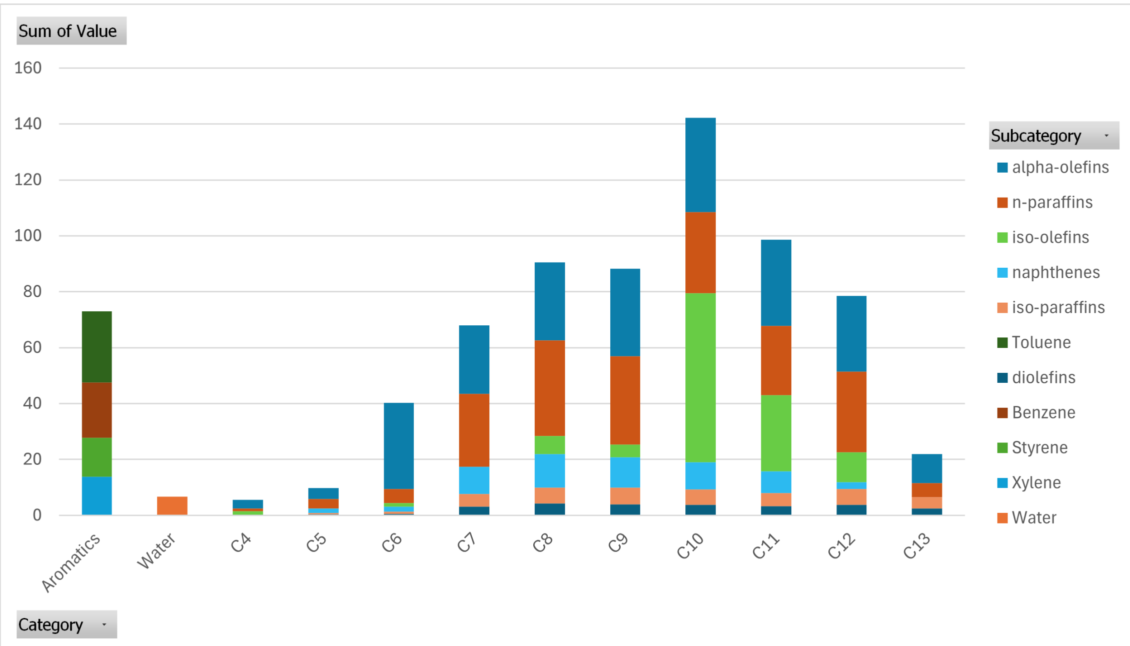

Figure B.5: Distribution of components from naphta product stream, process 3, PE feedstock.

B.1.3.3 Light gases

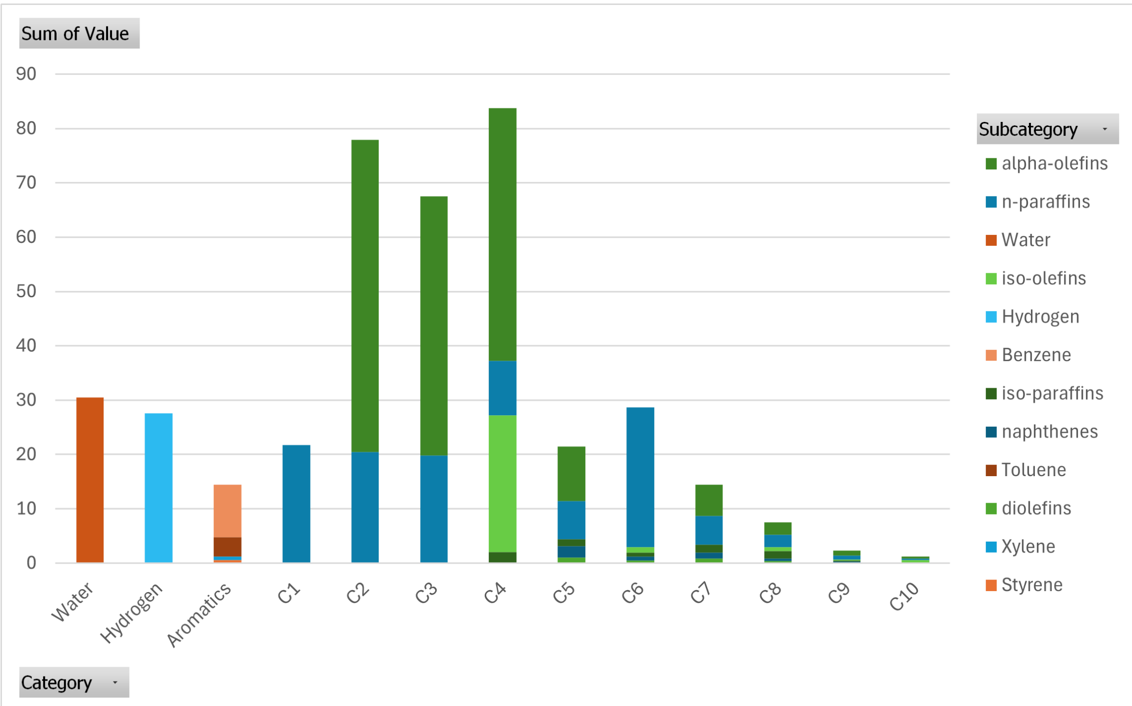

Figure B.6: Distribution of components from gas product stream, process 3, PE feedstock.

B.2 PP feedstock (Process 3)

B.2.1 Wax

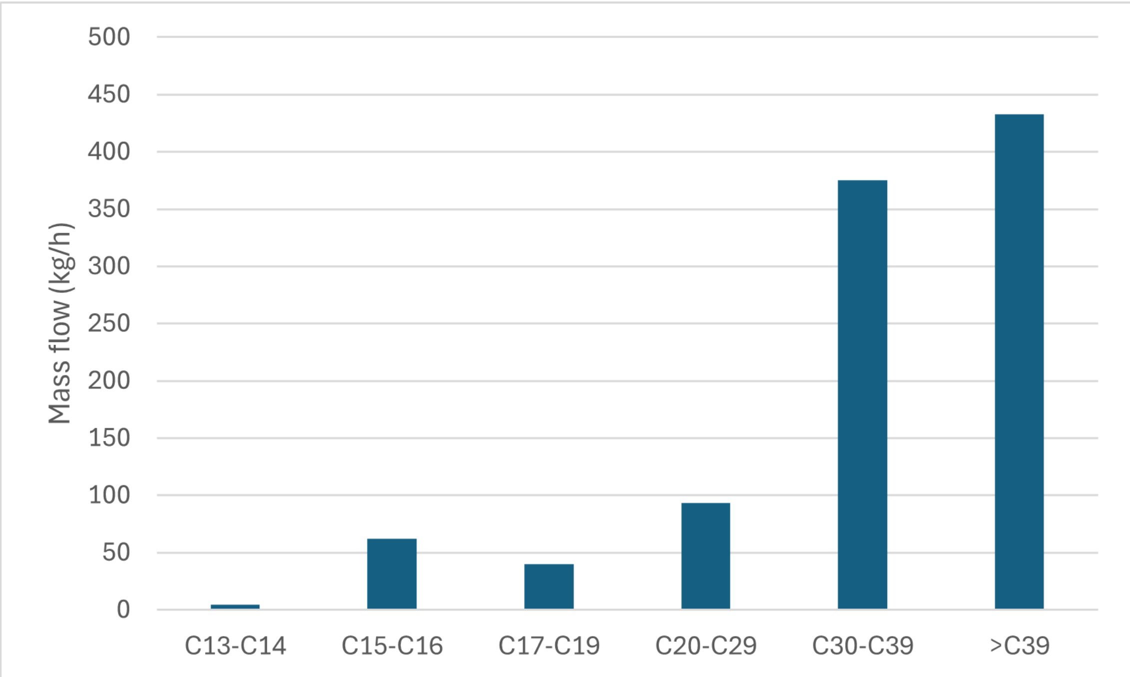

Figure B.7: Distribution of components from wax product stream, process 3, PP feedstock.

B.2.2 Diesel

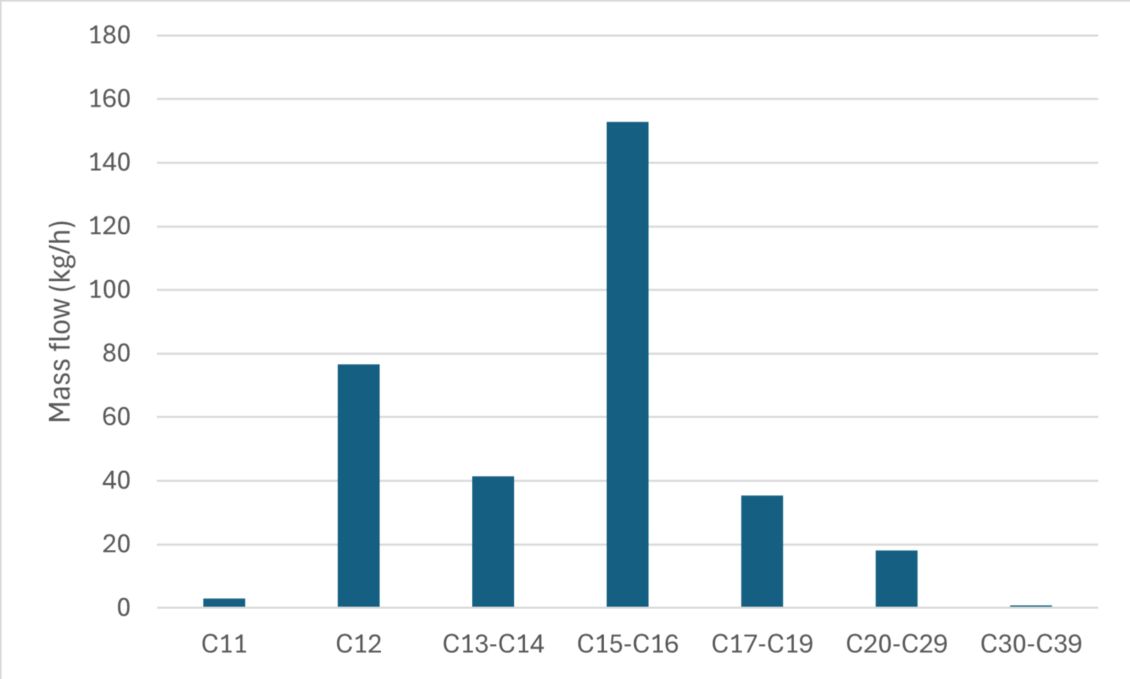

Figure B.8: Distribution of components from diesel product stream, process 3, PP feedstock.

B.2.3 Naphtha

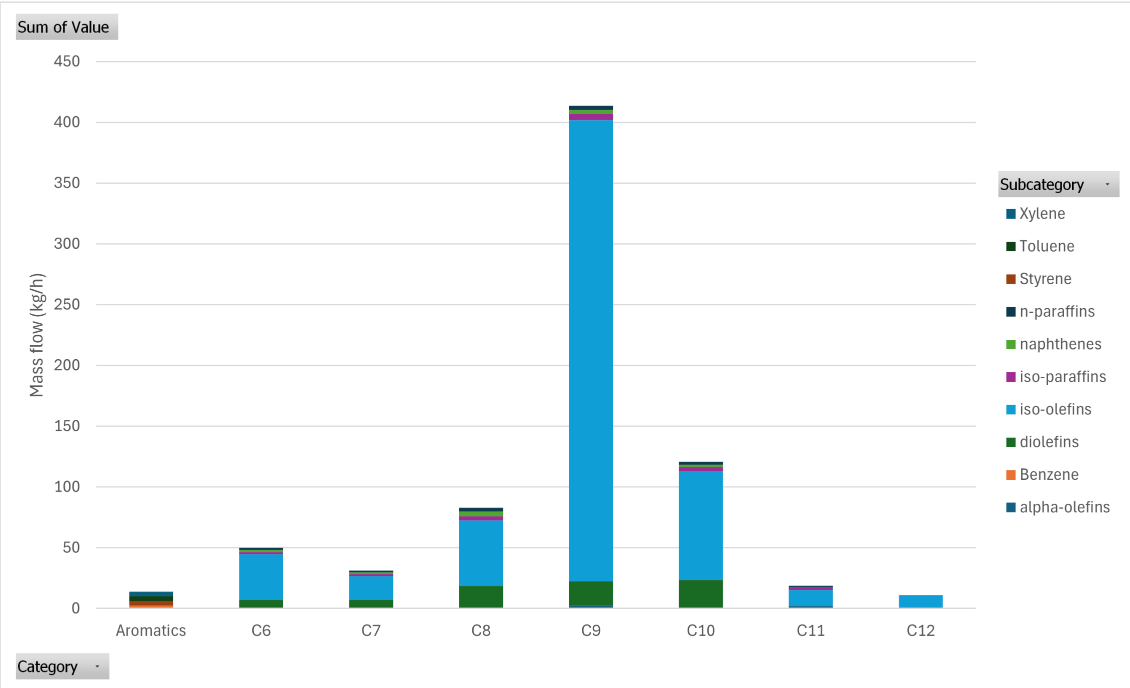

Figure B.9: Distribution of components from naphtha product stream, process 3, PP feedstock.

B.2.4 Light gases

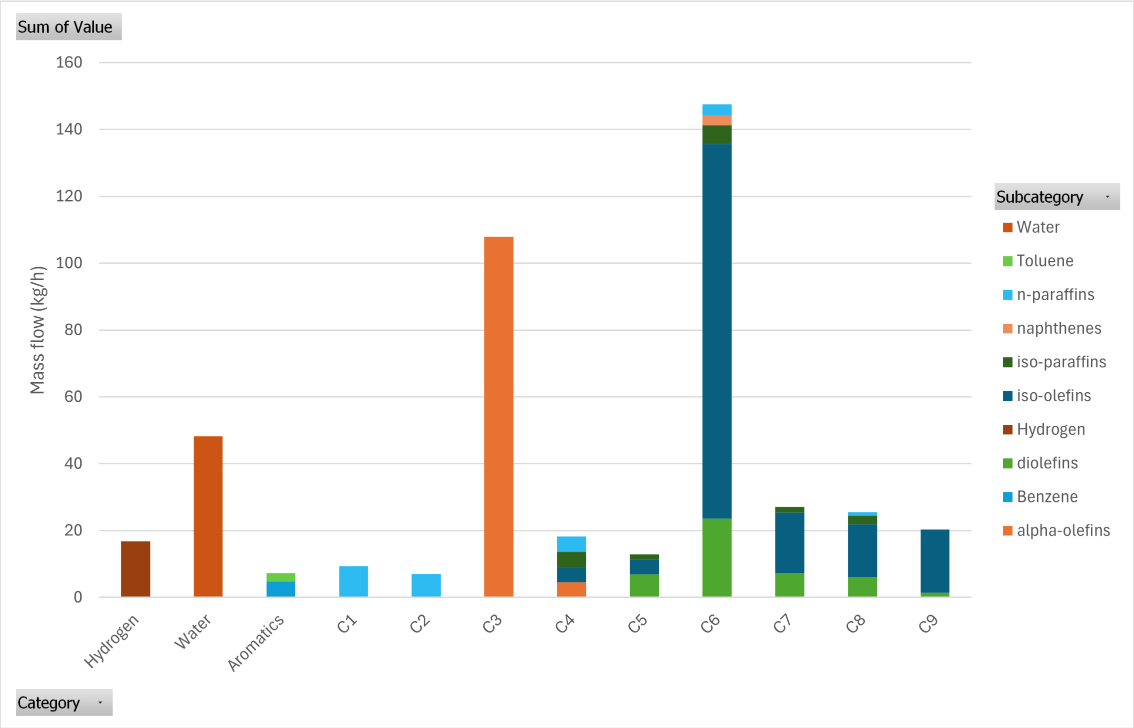

Figure B.10: Distribution of components from gas product stream, process 3, PP feedstock.

B.3 Mixed plastics feedstock (Process 3)

B.3.1 Wax

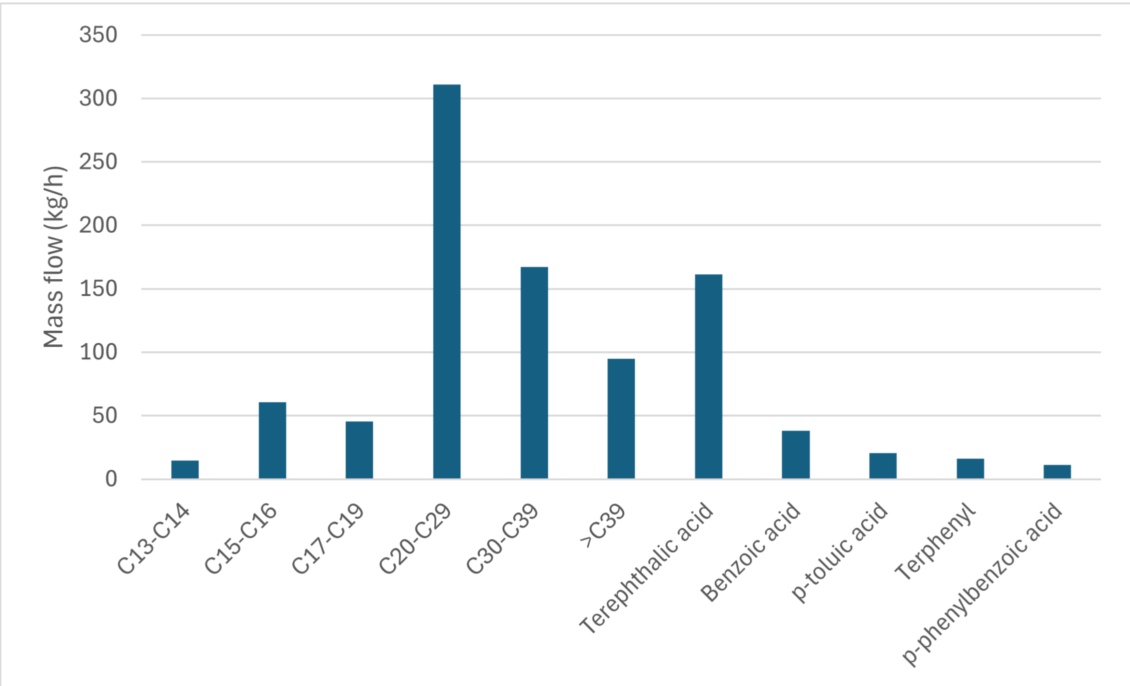

Figure B.11: Distribution of components from wax product stream, process 3, DKR-350 feedstock.

B.3.2 Diesel

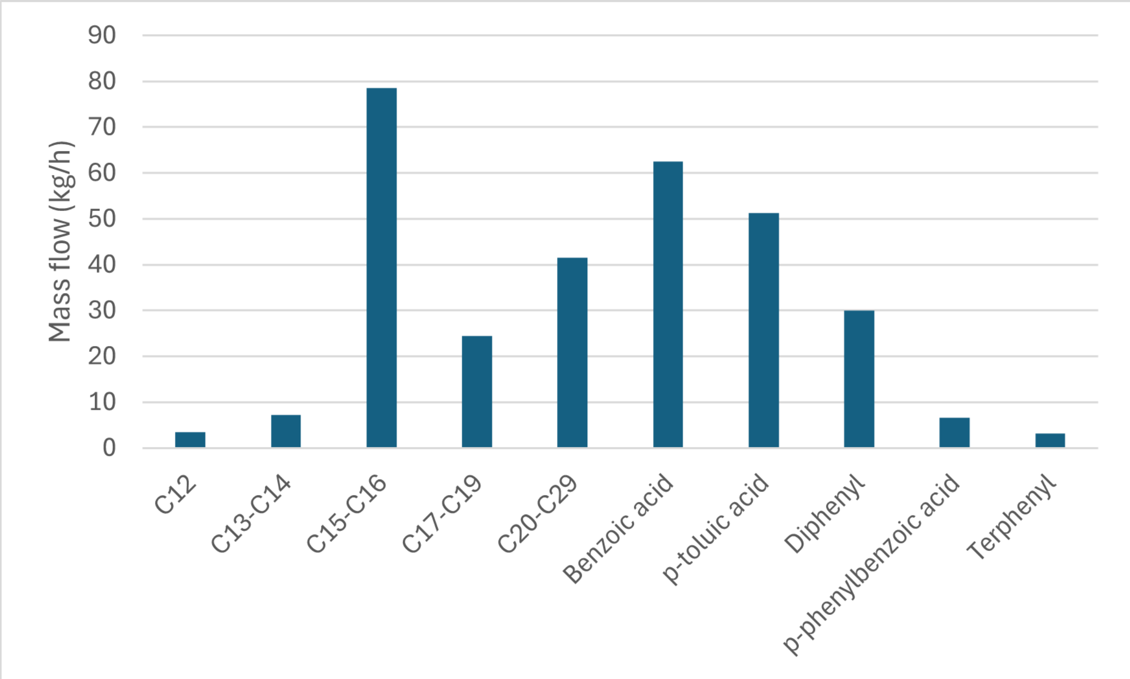

Figure B.12: Distribution of components from diesel product stream, process 3, DKR-350 feedstock.

B.3.3 Naphtha

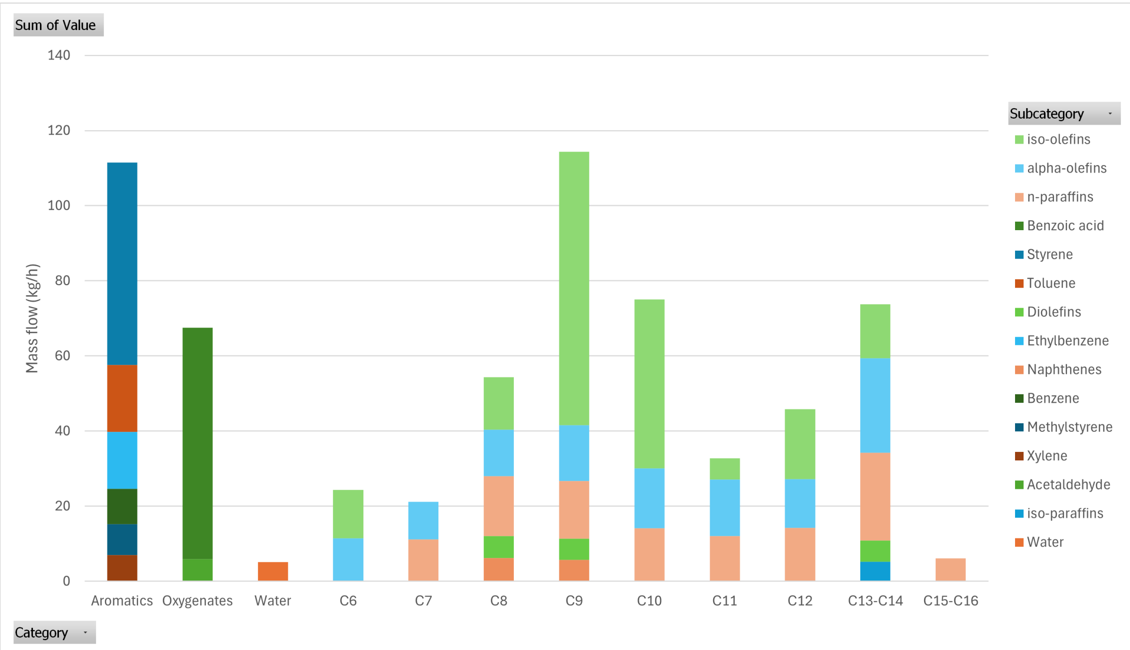

Figure B.13: Distribution of components from naphtha product stream, process 3, DKR-350 feedstock.

B.3.4 Light gases

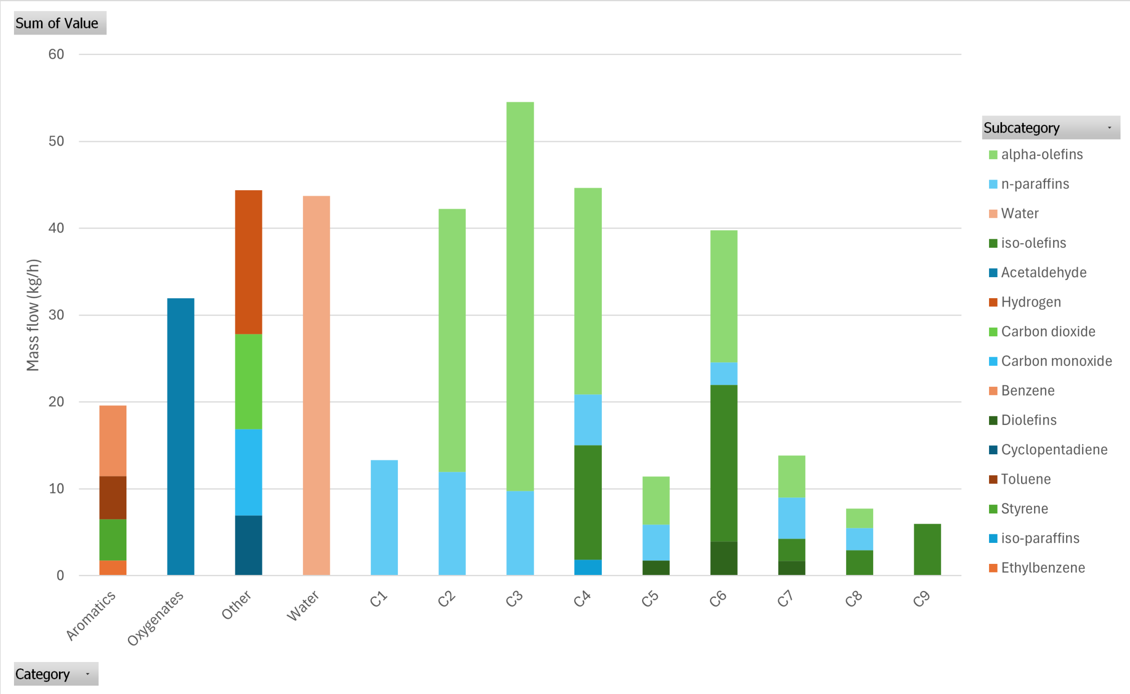

Figure B.14: Distribution of components from gas product stream, process 3, DKR-350 feedstock.

C
Economic assessment

C.1 Process 1

Table C.1: Equipment costs of process 1, in prices of 2010.

Equipment	Cost (USD)	Cost (MSEK)
Flash 1	$15 563	0,16
Flash 2	$14 977	0,15
Flash 3	$14 754	0,15
Heat exchangers	$6 794	0,07
Total	**$52 087**	**0,52**

Table C.2: Summary of capital costs of process 1, in prices of 2025.

Item	Cost (USD)	Cost (MSEK)
Total equipment cost	$78 194	0.78
Total capital cost	$304 959	3.05
Working capital (5% of Fixed Capital)	$15 248	0.15

Table C.3: Operating costs of process 1.

Fixed Operating Costs	SEK/year
Maintenance	91,488
Labour (8 staff, 2 per shift $\times$ 4 shifts)	5,568,000
Lab cost	1,224,960
Supervision	1,392,000
Management	2,784,000
Rate on capital	304,959
Insurance and taxes	30,496
Subtotal Fixed Costs	**11,395,903**
Variable Operating Cost	167,365
Total Operating Cost	**11,563,268**

C.2 Process 2

Table C.4: Equipment costs of process 2, in prices of 2010.

Equipment	Cost (USD)	Cost (MSEK)
Flash 1	$15,563	0.16
Flash 2	$14,977	0.15
Flash 3	$14,148	0.14
Flash 4	$13,709	0.14
Heat exchangers	$8,759	0.09
Total	**$67,155**	**0.67**

Table C.5: Summary of capital costs of process 2, in prices of 2025.

Item	Cost (USD)	Cost (MSEK)
Total equipment cost	$100 816	1.01
Total capital cost	$393 179	3.93
Working Capital (5% of Fixed Capital)	$19 659	0.20

Table C.6: Operating costs of process 2.

Fixed Operating Costs	SEK/year
Maintenance	117,954
Labour (8 staff, 2 per shift × 4 shifts)	5,568,000
Lab cost	1,224,960
Supervision	1,392,000
Management	2,784,000
Rate on capital	393,179
Insurance and taxes	39,318
Subtotal Fixed Costs	**11,519,411**
Variable Operating Cost	164,329
Total Operating Cost	**11,683,739**

C.3 Process 3

Table C.7: Equipment costs of process 3, in prices of 2010.

Equipment	Cost (USD)	Cost (MSEK)
Distillation column 1	$23,779	0.24
Distillation column 2	$14,204	0.14
Flash 1	$15,563	0.16
Flash 2	$14,977	0.15
Decanter	$15,357	0.15
Heat exchangers	$12,582	0.13
Total	**$96,462**	**0.96**

Table C.8: Summary of capital costs of process 3, in prices of 2025.

	US$	MSEK
Total equipment cost (prices of 2024)	$144,810	1.45
Total capital cost	$564,762	5.65
Working capital	$28,238	0.28

Table C.9: Operating costs of process 3.

Fixed Operating Costs	SEK/year
Maintenance	169,429
Labour	5,568,000
Number of staff (in shift positions): 8 (2 per shift, 4 shifts)	
Wages per employee: 40,000 SEK/month	
Allowance/Overhead factor: 1.45 → 58,000 SEK/month	
Total annual wage cost	696,000 per employee
Lab cost	1,224,960
Supervision	1,392,000
Management	2,784,000
Rate on capital	564,762
Insurance and taxes	56,476
Total Fixed Operating Costs	**11,759,627**
Variable Operating Cost	**161,271**
Total Operating Cost (SEK/year)	**11,920,898**

DEPARTMENT OF SPACE, EARTH AND ENVIRONMENT
CHALMERS UNIVERSITY OF TECHNOLOGY
Gothenburg, Sweden
www.chalmers.se

CHALMERS
UNIVERSITY OF TECHNOLOGY